Naval Research Laboratory
Washington, DC 20375-5000

NRL Memorandum Report 6527

Chemical Interactions and Light Emissions from Vented Species

P.A. BERNHARDT AND M.J. MULBRANDON

Geophysical and Plasma Dynamics Branch
Plasma Physics Division

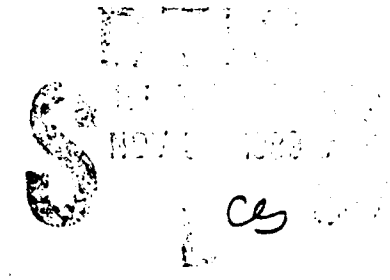

October 20, 1989

SECURITY CLASSIFICATION OF THIS PAGE

REPORT DOCUMENTATION PAGE

Form Approved
OMB No. 0704-0188

1a. REPORT SECURITY CLASSIFICATION UNCLASSIFIED	1b. RESTRICTIVE MARKINGS
2a. SECURITY CLASSIFICATION AUTHORITY	3. DISTRIBUTION / AVAILABILITY OF REPORT Approved for public release; distribution unlimited.
2b. DECLASSIFICATION / DOWNGRADING SCHEDULE	
4. PERFORMING ORGANIZATION REPORT NUMBER(S) NRL Memorandum Report 6527	5. MONITORING ORGANIZATION REPORT NUMBER(S)
6a. NAME OF PERFORMING ORGANIZATION Naval Research Laboratory 6b. OFFICE SYMBOL (If applicable) Code 4780.1B	7a. NAME OF MONITORING ORGANIZATION
6c. ADDRESS (City, State, and ZIP Code) Washington, DC 20375-5000	7b. ADDRESS (City, State, and ZIP Code)
8a. NAME OF FUNDING / SPONSORING ORGANIZATION Lockheed 8b. OFFICE SYMBOL (If applicable) 0/92-20, B/255	9. PROCUREMENT INSTRUMENT IDENTIFICATION NUMBER
8c. ADDRESS (City, State, and ZIP Code) Palo Alto, CA 94305	10. SOURCE OF FUNDING NUMBERS PROGRAM ELEMENT NO. / PROJECT NO. / TASK NO. / WORK UNIT ACCESSION NO

11. TITLE (Include Security Classification)
Chemical Interactions and Light Emissions from Vented Species

12. PERSONAL AUTHOR(S)
Bernhardt, P.A. and Mulbrandon, M.J.

13a. TYPE OF REPORT	13b. TIME COVERED	14. DATE OF REPORT (Year, Month, Day)	15. PAGE COUNT
Final	FROM 6/88 TO 3/89	1989 October 20	46

16. SUPPLEMENTARY NOTATION

17. COSATI CODES			18. SUBJECT TERMS (Continue on reverse if necessary and identify by block number)
FIELD	GROUP	SUB-GROUP	Ionospheric modification, Ultraviolet emissions, Infrared emissions, Vehicle outgassing, Visible emissions

19. ABSTRACT (Continue on reverse if necessary and identify by block number)

The intensities of light emissions produced by the release of H_2O and CH_3OH into the upper atmosphere is estimated with a numerical mode. Chemical reactions between the injected neutrals, background ions, electrons, and neutrals, and artificially created ions and neutrals are considered. We find that OH is the primary excited species resulting from the water release. Vibrational and electronic states of OH will be excited to yield emission spectra between 240 and 4400 nm wavelengths. For the release of 10^{26} molecules in the nighttime ionosphere with a density of 10^6 cm^{-3}, the intensities of the emissions will be greater than 10^4 Rayleighs. The water release also produces vibrational states of H_2O and electronic states of atomic oxygen. The addition of methyl alcohol to the release causes substantial production of vibrationally excited formaldehyde. We conclude that the venting of reactive molecules into the upper atmosphere at 300 km altitude or above can produce excited species by neutral-neutral, ion-neutral, or electron-ion reactions. No one reaction process is dominant in the F-region.

20. DISTRIBUTION / AVAILABILITY OF ABSTRACT ☒ UNCLASSIFIED/UNLIMITED ☐ SAME AS RPT ☐ DTIC USERS	21. ABSTRACT SECURITY CLASSIFICATION UNCLASSIFIED
22a. NAME OF RESPONSIBLE INDIVIDUAL Paul A. Bernhardt	22b. TELEPHONE (Include Area Code) (202) 767-0196 22c. OFFICE SYMBOL Code 4780.1B

DD Form 1473, JUN 86 *Previous editions are obsolete.* SECURITY CLASSIFICATION OF THIS PAGE

S/N 0102-LF-014-6603

CONTENTS

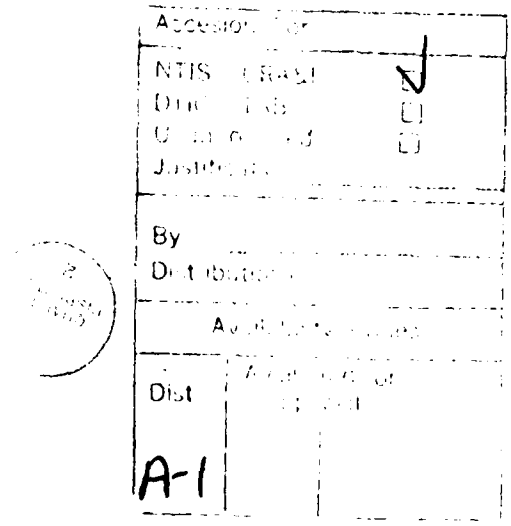

CHEMICAL INTERACTIONS AND LIGHT EMISSIONS FROM VENTED SPECIES

I. INTRODUCTION

Airglow emissions may be induced by the interaction of atmospheric constituents with vapors released from space vehicles. Such emissions can be produced by a number of chemical mechanisms. Previous studies have considered neutral-neutral energetic reactions as the causative mechanism for vibrational or electronic excitation of molecular species [Fraser et al., 1988]. This study considers neutral-plasma reactions as well as neutral-neutral reactions as the sources for excited species. To provide an example of the type of interactions which can occur, we model the chemical reactions and subsequent emissions resulting from water (H_2O) and methyl alcohol (CH_3OH) outgassed from a spacecraft in the upper atmosphere above 300 km altitude. The plasma interactions involve O^+ and H^+ thermal ions and low energy (<0.2 eV) electrons of ionospheric origin. Line and continuum emissions extending from the infrared to the extreme ultraviolet are of interest. The examples in this study are restricted to releases of a few kilograms. The techniques described here can be extended to determine the emissions caused by the release of materials besides H_2O and CH_3OH.

Manuscript approved August 7, 1989.

II. CHEMICAL REACTIONS

A released species initially reacts with O^+ or H^+ ions to produce a positive-ion-intermediary (PII) [Bernhardt, 1987]. The PII's are destroyed by a dissociative recombination reaction which may yield excited species which subsequently decay by the emission of a photon. The complete process is summarized by the reactions:

$$XY + Z^+ \rightarrow XZ^+ + Y \qquad \text{rate: } k_1 \sim 10^{-9} \text{ cm}^3/\text{s} \qquad (1)$$

$$XZ^+ + e^- \rightarrow X^* + Z \qquad \text{rate: } k_2 \sim 10^{-7} \text{ cm}^3/\text{s} \qquad (2)$$

$$X^* \rightarrow X + h\nu \qquad \text{rate: } A \sim 10^{-3} \text{ to } 10^6 \text{ s}^{-1} \qquad (3)$$

where XY is a generic symbol for the released chemical, Z^+ represents O^+ or H^+, XZ^+ is the positive ion intermediary and X^* is the excited species which radiates a photon $h\nu$.

A. Ion-Molecule Reactions

The primary ion-molecule reactions for the ionospheric releases are

$$O^+ + H_2O \rightarrow H_2O^+(v \leq 6) + O + 1.02 \text{ eV} \qquad k_{1A} = 2.4 \times 10^{-9} \qquad (4)$$

$$H^+ + H_2O \rightarrow H_2O^+(v \leq 6) + H + 1.00 \text{ eV} \qquad k_{1B} = (2.4 \times 10^{-9}?) \qquad (5)$$

$$\begin{aligned} O^+ + CH_3OH &\rightarrow CH_3O^+ + OH(v) + ? \text{ eV} \quad (70\%) \\ &\rightarrow CH_3OH^+ + O^* + 2.78 \text{ eV} \quad (25\%) \\ &\rightarrow CH_2O^+ + H_2O + 6.90 \text{ eV} \quad (5\%) \end{aligned} \qquad k_{1C} = 1.9 \times 10^{-9} \qquad (6)$$

$$\begin{aligned} H^+ + CH_3OH &\rightarrow CH_3O^+ + H_2 \\ &\rightarrow CH_4^+ + OH(v \leq 2) + 1.5 \text{ eV} \\ &\rightarrow CH_3OH^+ + H + 2.76 \text{ eV} \end{aligned} \qquad k_{1D} = (1.9 \times 10^{-9}?) \qquad (7)$$

The rate constants (in cm^3/s) are from laboratory studies at temperatures of 300 K [Albritton, 1878; Ikezoe et al., 1987]. The (O^+, H_2O) reaction rate (k_{1A}) is nearly constant for energies up to 5 eV [Murad, private

communication, 1988].

Secondary ion-molecule reactions occur between the reaction products and the injected or background species.

$$H_2O^+ + H_2O \rightarrow H_3O^+ + OH(v\leq 2) + 1.17\ eV \qquad k_{1E} = 1.67 \times 10^{-9} \qquad (8)$$

$$H_2O^+ + O_2 \rightarrow O_2^+ + H_2O + 0.54\ eV \qquad k_{1F} = 4.3 \times 10^{-10} \qquad (9)$$

$$O^+ + OH \rightarrow OH^+(v\leq 1) + O + 0.45\ eV \qquad k_{1G} \sim 1.6 \times 10^{-9} \qquad (10)$$

$$O^+ + H_2 \rightarrow OH^+(v\leq 1) + H + 0.37\ eV \qquad k_{1H} = 2.0 \times 10^{-9} \qquad (11)$$

$$O^+ + CH_2O \rightarrow CHO^+ + OH(v\leq 9) + 4.49\ eV\ (40\%) \qquad k_{1I} = 3.5 \times 10^{-9} \qquad (12)$$
$$\rightarrow CH_2O^+ + O^* + 2.74\ eV\ (60\%)$$

$$O^+ + CH_4 \rightarrow CH_4^+ + O + 1.01\ eV\ (89\%) \qquad k_{1J} = 1.0 \times 10^{-9} \qquad (13)$$
$$\rightarrow CH_3^+ + OH(v\leq 9) + 3.78\ eV\ (11\%)$$

$$O^+ + CH_3 \rightarrow CH_3^+ + O^* + 3.77\ eV \qquad k_{1K} = 1.0 \times 10^{-9} \qquad (14)$$

$$O^+ + CH_2 \rightarrow CH_2^+ + O^* + 3.22\ eV \qquad k_{1L} = 1.0 \times 10^{-9} \qquad (15)$$

$$O^+ + CH \rightarrow CH^+ + O^* + 2.49\ eV \qquad k_{1M} = 1.0 \times 10^{-9} \qquad (16)$$

$$H_3O^+ + CH_3OH \rightarrow CH_5O^+ + H_2O \qquad k_{1N} = 2.2 \times 10^{-9} \qquad (17)$$

$$CH_3O^+ + H_2O \rightarrow H_3O^+ + CH_2O(v) \qquad k_{1O} = 2.3 \times 10^{-9} \qquad (18)$$

$$CH_2O^+ + H_2O \rightarrow H_3O^+ + CHO + 0.8\ eV \qquad k_{1P} = 2.6 \times 10^{-9} \qquad (19)$$

$$CH_4^+ + H_2O \rightarrow H_3O^+ + CH_3 + 1.87\ eV \qquad k_{1Q} = 2.6 \times 10^{-9} \qquad (20)$$

$$CH_4^+ + CH_3OH \rightarrow CH_4O^+ + CH_4 + 1.8\ eV\ (60\%) \qquad k_{1R} = 3.0 \times 10^{-9} \qquad (21)$$
$$\rightarrow CH_5O^+ + CH_3 \qquad (40\%)$$

$$CH_3OH^+ + CH_3OH \rightarrow CH_5O^+ + CH_3O \qquad k_{1S} = 2.5 \times 10^{-9} \qquad (22)$$

$$CH_5O^+ + CH_3OH \rightarrow H^+ \cdot CH_3OCH_3 + H_2O \qquad k_{1T} = 1.0 \times 10^{-10} \qquad (23)$$

where all rate constants are in cm^3/s. For all ion-molecule reactions which may yield excited oxygen (O^*), it is assumed that 10% is in the metastable $O(^1D)$ state and that 90% is in the ground $O(^3P)$ state. The value for k_{1G} in (10) is an estimate based on similar reactions.

If known, the excess energy of each reaction is indicated. If this energy is much less than the injection kinetic energy relative to O^+ or H^+, then the reaction rates may be significantly different than the thermal rates shown. For injection velocities less than 5 km/s, the kinetic energy of O^+ is less than 2.08 eV and of H^+ is less than 0.13 eV. All of the chemical rate constants k_{1A} through k_{1H} are valid for these energies.

The excess energy also indicates which species may be electronically excited. The energy of reaction plus the orbital kinetic energy may combine to leave the reaction products in excited states not attainable from low energy releases.

B. Dissociative Recombination Reactions

The amount of energy released during dissociative recombination is given by $E_o = I(XZ) - D(XZ)$ where I and D are the respective ionization potential and dissociation energy of molecule XZ in reaction (2). The ion-electron reactions for the modified plasma are

$$\begin{aligned} H_2O^+ + e^- &\rightarrow OH(X^2\Pi_i, v \leq 9) + H + 7.45 \text{ eV} \quad (55\%) \\ &\rightarrow OH(A^2\Sigma^+, v \leq 9) + H + 3.40 \text{ eV} \\ &\rightarrow O(X^3P) + H_2 + 7.64 \text{ eV} \\ &\rightarrow O(A^1D) + H_2 + 5.67 \text{ eV} \quad (10\%) \quad k_{2A} = 6.5 \times 10^{-7} \\ &\rightarrow O(B^1S) + H_2 + 3.00 \text{ eV} \end{aligned} \qquad (24)$$

$\rightarrow O(X^3P) + 2H + 3.00$ eV (35%)
$\rightarrow O(A^1D) + 2H + 1.03$ eV

$H_3O^+ + e^- \rightarrow H_2O(X^1A_1, v) + H + 6.29$ eV (14%)

$\rightarrow OH(X^2\Pi_i, v \leq 9) + H_2 + 5.63$ eV (74%) $k_{2B} = 6.3 \times 10^{-7}$ (25)
$\rightarrow OH(A^2\Sigma^+, v \leq 5) + H_2 + 1.58$ eV

$\rightarrow OH(X^2\Pi_i, v \leq 2) + 2H + 1.09$ eV (12%)

$O_2^+ + e^- \rightarrow O^* + O^* + 6.90$ eV $k_{2C} = 1.9 \times 10^{-7}$ (26)

$OH^+ + e^- \rightarrow O^* + H + 8.74$ eV $k_{2D} = 7.5 \times 10^{-8}$ (27)

$CHO^+ + e^- \rightarrow CO^* + H + 7.72$eV $k_{2E} = 1.1 \times 10^{-7}$ (28)

$CH_2O^+ + e^- \rightarrow CHO + H + 7.11$ eV $k_{2F} = ?$ (29)

$CH_3O^+ + e^- \rightarrow CH_2O(v) + H$ $k_{2G} = ?$ (30)

$CH_3OH^+ + e^- \rightarrow CH_2O(v) + H_2 + 9.92$ eV
$\rightarrow CH_2O(v) + H + H + 5.4$ eV $k_{2H} = ?$ (31)
$\rightarrow CH_2 + H_2O^* + 6.83$ eV

$CH_5O^+ + e^- \rightarrow CH_4 + OH$ $k_{2I} = 8.8 \times 10^{-7}$ (32)

$C_2H_7O^+ + e^- \rightarrow C_2H_6O + H$ $k_{2J} = ?$ (33)

$CH_4^+ + e^- \rightarrow CH_3 + H + 8.16$ eV (50%) $k_{2K} = 8.0 \times 10^{-7}$ (34)
$\rightarrow CH_2 + H_2 + 7.90$ eV (50%)

$CH_3^+ + e^- \rightarrow CH_2 + H + 4.99$ eV (50%) $k_{2L} = 8.0 \times 10^{-7}$ (35)
$\rightarrow CH + H_2 + 5.08$ eV (50%)

$CH_2^+ + e^- \rightarrow CH + H + 6.03$ eV $k_{2M} = 6.0 \times 10^{-7}$ (36)

$CH^+ + e^- \rightarrow C + H + 7.63$ eV $k_{2N} = 4.0 \times 10^{-7}$ (37)

where the rate constants (cm^3/s) all scale as $(300/T_e)^{1/2}$, T_e is the electron temperature and the unknown rate constants have values around 6 x 10^{-7} cm^3/s [Mitchell and McGowan, 1983]. The percentages for the products for dissociative recombination of H_2O^+ and H_3O^+ are taken from Rowe et al. [1988] and Herbst [1978], respectively. The species which may be vibrationally or electronically excited are designated by "v" or "*", respectively. For reaction (24), we assume a 10% yield of $O(^1D)$. Reaction (26) produces oxygen in the $O(^1S)$, $O(^1D)$ and $O(^3P)$ states with respective branching ratios of 0.1, 0.9, and 1.0 [Zipf, 1970 and Zipf, 1980]. By analogy, we assume that (27) yields atomic oxygen with branching ratios of 0.05, 0.45, and 0.50.

C. Neutral-Neutral Reactions

Even though this study concentrates on interactions between the plasma and the injected neutrals, neutral chemistry cannot be neglected. The neutral ambient atmosphere between 300 and 3000 km altitude is composed of potentially reactive species such as O, N_2, O_2, and H. Reactions between atomic oxygen and the released gases are

$$O + H_2O \rightarrow OH + OH - 0.73 \text{ eV} \qquad k_{3A} = 6.0 \times 10^{-15} \qquad (38)$$

$$O + H_2O(v) \rightarrow OH + OH \qquad k'_{3A} = 1 \times 10^{-11}$$

$$O + CH_3OH \rightarrow H_2O(v) + CH_2O(v) + 4.28 \text{ eV} \qquad k_{3B} = 8.5 \times 10^{-13} \qquad (39)$$

All of the reactions for this section are given by Schofield [1967] and Kondratiev [1972] for neutral temperatures of 1000 K. Reaction (38) is

endothermic and, consequently, slow at thermospheric temperatures. The rate constant for reaction of H_2O with atomic oxygen is about 10^6 times slower than the rate of H_2O reacting with O^+ in (4). Above 300 km altitude, the ratio O^+ to O concentration is 10^{-4} or greater. Therefore, thermal interactions between O and H_2O are unimportant.

For vibrationally excited water, the rate constant for (38) becomes $k'_{3A} = 1.0 \times 10^{-11}$. A similar rate increase occurs for neutral H_2O moving at orbital velocities relative to the ambient atmosphere. At 5 km/s, the center of mass energy is 2.0 eV and the reaction cross section for (38) is approximately 1×10^{-7} cm^2 [Fraser et al., 1988]. In this study, we will neglect the high energy reaction chemistry and only consider low-speed, thermal reactions.

Reaction between atomic oxygen and water vapor will be greatly enhanced for excited states. For example, metastable oxygen reacts rapidly with H_2O

$$O(^1D) + H_2O \rightarrow OH(v) + OH(v) + 1.23 \text{ eV} \qquad k_{3C} = 2.0 \times 10^{-10} \qquad (40)$$

where OH can be produced in the v=0,1,or 2 vibrational states.

Reaction (39) is exothermic under all conditions. It is dominant where $k_{3B}[O]$ is greater than or equal to the quantity $k_{1C}[O^+]$. The reaction products of (39) are in vibrational states which will emit infrared radiation.

The following neutral reactions help determine the fate of the products from the ion-molecule and dissociative-recombination reactions:

$$O + OH \rightarrow O_2^* + H + 0.73 \text{ eV} \qquad k_{3D} = 5.0 \times 10^{-11} \qquad (41)$$
$$O + OH(v) \rightarrow O_2^* + H$$

$$OH + OH \rightarrow H_2O(v) + O + 0.73\ eV \qquad k_{3E} = 2.0 \times 10^{-12} \qquad (42)$$

$$OH(v) + OH(v) \rightarrow H_2O(v) + O \qquad k'_{3E} = 3.0 \times 10^{-11}$$

$$OH + CH_4 \rightarrow CH_3 + H_2O + 0.75\ eV \qquad K_{3F} = 3.0 \times 10^{-11} \qquad (43)$$

$$O + CH_3 \rightarrow CH_2O(v) + H + 3.00\ eV \qquad k_{3G} = 3.0 \times 10^{-11} \qquad (44)$$

$$OH(v) + \{O_2 \text{ or } N_2\} \rightarrow OH(v-1) + \{O_2 \text{ or } N_2\} \qquad k_{3H} = v \times 8 \times 10^{-13} \qquad (45)$$

Both (41) and (42) can produce significant reductions in the OH concentrations. The rate constants for vibrational relaxation of OH in reactions (41), (42) and (45) are provided by Llewellyn et al. [1978].

No other neutral reactions are used in the model because either the reactions are slow or, for H and O_2, the background concentrations are low.

III. EMISSIONS FROM EXCITED SPECIES

For the water release, the most likely sources of enhanced emissions are H_2O^+ [reactions (4) or (5)], OH [reactions (8), (12), (13), (24), or (25)], and H_2O [reaction (20)]. Many bands of the $A^2A_1 \rightarrow X^2B_1$ electron emission spectrum of H_2O^+ occurring in the 4000-7000 Angstrom wavelength region have been analyzed [Lew, 1976]. These include bands which have been seen in the tails of comets but were not seen during the low-velocity H_2O releases (called Lagopedo) conducted over Hawaii in 1977.

Observations of the 3064 A emission from the lowest-energy, vibronic state of OH were reported by Yau et al. [1985] from the H_2O release during Waterhole I. The emission reaction is $OH(A^2\Sigma) \rightarrow OH(X^2\Pi) + h\nu(3064\ A)$ where both the initial and final states are in the v = 0 vibrational state. The

emission intensity was about 10^3 Rayleigh. Only 5% of the OH in reaction (24) was formed in the $^2\Sigma$ state [Anderson and Bernhardt, 1978]. The important emission bands from $OH(A^2\Sigma)$ and their spontaneous emission rates are shown in Table I. The initial and final vibrational levels are indicated by (v', v") [Crosley and Lengel, 1975].

Table I

Vibronic Transitions between $OH(A^2\Sigma^+)$ v' and $OH(X^2\Pi_i)$ v"

(Wavelengths in Angstroms and $A_{v',v"}$ in s^{-1})

v' \ v"	0	1	2	3	4
0	3064 1.2×10^6	3428 4.4×10^6			
1	2811 2.1×10^6	3122 1.3×10^6	3484 1.4×10^4		
2	2609 4.2×10^5	2875 3.3×10^6	3185 1.8×10^6	3550 2.2×10^4	
3	2444 1.4×10^4	2677 1.7×10^5	2945 5.5×10^5	3254 2.6×10^5	3353 ?
4		2517 ?	2753 ?	3022 ?	3331 ?

The ground state of $OH(X^2\Pi)$ can be vibrationally excited by reactions (7), (8), (24), and (25). The vibrational and rotational bands for the ground state of OH extend from 44745 to 3810 Angstroms as shown in Table II. The vibrational transition probabilities have been theoretically derived by Mies [1974]. We may be able to estimate the intensities of the OH lines by comparison with the well known reaction of ozone with atomic hydrogen $O_3+H\rightarrow O_2+OH^*+3.40$ eV [McDade and Llewellyn, 1988].

Table II

Vibrational Transitions in the $OH(X^2\Pi_i)$ state (Angstroms)

v' \ v"	0	1	2	3	4	5	6	7	8
1	28016								
2	14342	29380							
3	9791	15052	30862						
4	7461	10286	15830	32495					
5	6137	7849	10684	16690	34308				
6	5254	6464	8278	11285	17647	36334			
7	4627	5542	6827	8758	11961	18734	38668		
8	4164	4890	5865	7239	9305	12743	20003	41440	
9	3810	4409	5187	6234	7712	9942	13662	21514	44745

Transition Probabilities for $OH(X^2\Pi_i)$ (s^{-1})

v' \ v"	0	1	2	3	4	5	6	7	8
1	20.00								
2	13.98	25.23							
3	0.91	39.63	21.35						
4	0.08	4.27	72.02	13.47					
5	0.05	0.39	10.56	107.4	06.79				
6	0.00	0.05	1.27	20.88	139.90	6.03			
7	0.00	0.00	0.18	2.88	37.18	161.0	14.32		
8	0.00	0.00	0.03	0.56	5.64	60.62	163.7	32.41	
9	0.00	0.00	0.00	0.13	1.16	10.81	89.86	143.1	58.12

The excitation of atomic oxygen by reaction (27) has been not been verified by laboratory or space experiments. It is likely, however, that the metastable $O(^1D)$ and $O(^1S)$ will be produced. These states radiate visible emissions by the following reactions:

$$O(^1D) \rightarrow O(^3P) + h\nu(6300\ A) \qquad A_1 = 5.1 \times 10^{-3}\ s^{-1} \qquad (46)$$

$$O(^1D) \rightarrow O(^3P) + h\nu(6363\ A) \qquad A_2 = 1.6 \times 10^{-3}\ s^{-1} \qquad (47)$$

$$O(^1S) \rightarrow O(^1D) + h\nu(5577\ A) \qquad A_3 = 1.34\ s^{-1} \qquad (48)$$

Quenching of $O(^1D)$ by collisions with molecules (N_2, O_2, H_2O, etc.) is represented by the reaction:

$$O(^1D) + N_2 \rightarrow O(^3P) + N_2^* \qquad k_Q = 3.0 \times 10^{-11}\ cm^3/s \qquad (49)$$

and by (40).

The H_2O excitation by reaction (25) has not been experimentally verified. From energy considerations, we know that this reaction may only yield ground state $H_2O(X^1A_1)$ because the next highest level is a triplet state which requires an energy greater than 6.5 eV for excitation [Wang et al., 1977]. The $H_2O(X^1A_1)$ vibrational levels are given by the formula

$$G(v_1,v_2,v_3) = \omega_1 v_1 + \omega_2 v_2 + \omega_3 v_3 + X_{11} v_1^2 + X_{22} v_2^2 + X_{33} v_3^2 + X_{12} v_1 v_2 + X_{13} v_1 v_3 + X_{23} v_2 v_3 \qquad (50)$$

where v_1, v_2, and v_3 are the vibrational quantum numbers and the coefficient values (cm^{-1}) are

$$\omega_1 = 3693.8 \quad \omega_2 = 1614.5 \quad \omega_3 = 3801.7$$
$$X_{11} = -43.8 \quad X_{22} = -19.5 \quad X_{33} = -46.3$$
$$X_{12} = -20.0 \quad X_{13} = -155.0 \quad X_{23} = -19.8$$

The H_2O spectrum is found from the difference in energy levels by the formula

$$\lambda(\text{Angstroms}) = 10^8/[G(v_1',v_2',v_3') - G(v_1'',v_2'',v_3'')] \qquad (51)$$

The H_2O emission bands and their associated excitation energy are given in Table III.

Table III

H_2O Emission Bands

$(v_1,v_2,v_3) \rightarrow (0,0,0)$ Transitions

Wavelength (A)	v_1	v_2	v_3	Energy (eV)	Spectral Range (A)
62696	0	1	0	0.198	
31732	0	2	0	0.391	
27385	1	0	0	0.453	
26625	0	0	1	0.466	
18755	0	1	1	0.661	
14548	0	2	1	0.852	
13790	1	0	1	0.899	
11355	1	1	1	1.092	
9422	2	0	1	1.316	
9064	0	0	3	1.367	
8230	2	1	1	1.507	7993 to 8448
7959	0	1	3	1.558	7846 to 8093
7230	3	0	1	1.715	7059 to 7408
6984	1	0	3	1.775	6845 to 7128
6516	3	1	1	1.903	6408 to 6626
6316	1	1	3	1.963	6275 to 6375
5945	3	2	1	2.086	5828 to 6019
5918	4	0	1	2.095	5830 to 5999
5716	2	0	3	2.169	5665 to 5769

The transition probabilities for the ground vibrational states of H_2O are given in Table IV.

The emissions form the methyl alcohol vapors will most likely come from chemical excitation of formaldehyde (CH_2O) by reactions (18), (30), and (31). The transition probabilities for the six fundamental vibrational states of CH_2O are given in Table IV.

Table IV

Transition Probabilities of Vibrationally Excited Molecules

Molecule	Vibrational State	Fundamental Wavelength ν_i (A)	Transition Probability $A_{v',v''}$ (s^{-1})
H_2O	$3(B_1)$	26625	76
	$2(A_1)$	62696	16
CH_2O	$6(B_2)$	79554	2.0
	$5(B_2)$	35125	130
	$4(B_1)$	84746	1.7
	$3(A_1)$	66357	2.6
	$2(A_1)$	57208	22
	$1(A_1)$	35971	124

IV. CONTINUITY EQUATIONS

The ionospheric perturbations and airglow enhancements can be estimated by solving coupled continuity equations for the ions and neutrals. The diffusion equation for the neutrals is

$$\frac{\partial n}{\partial t} = \nabla\cdot(D\nabla n) + P - L \tag{52}$$

where n is the neutral gas concentration, D is the diffusion coefficient, P and L are the production and loss terms representing the chemical reactions. The depletion of the injected gas by diffusion is much more rapid than the depletion by chemical reactions [Bernhardt, 1979]. For that case, P and L can be neglected and the analytic solution to (52) can be written as

$$n = \frac{N_o}{(4\pi Dt)^{3/2}} \exp(-r^2/4Dt) \tag{53}$$

where N_o is the number of H_2O or CH_3OH molecules released and r is the distance from the center of a point release.

Initially, our model will neglect diffusion of the reaction products from the chemical reactions. This typically yields a factor of two overestimate in the airglow intensities [Bernhardt, 1984]. The coupled set of rate equations for the densities are of the form

$$\frac{\partial n_i}{\partial t} = F_i(n_1, n_2, \ldots, n_J) \quad \text{for } i=1,2, \ldots,J \tag{54}$$

where n_i is the density of species number "i" and F_i is the production and loss function representing chemical interactions with all of the densities, and J is the total number of species to be calculated.

The intensity is calculated with a line of sight integral of the volume emission rate. In Rayleighs, the intensity is found from

$$I = 10^{-6} \int_{-\infty}^{\infty} A\, n\, dr \tag{55}$$

where A is the Einstein coefficient of the desired transition of excited species n.

The time dependent equations are solved using the program CHEMGLOW developed at NRL. Equation (54) is solved in steady state for reactions with fast time constants ($\sim 10^{-3}$ sec or less). The inputs to the program are background neutral and ion densities, background temperatures, and number of H_2O and CH_3OH molecules released. The outputs are temporal variations in densities of ions and excited species, and in airglow emission intensities. The program is written in Fortran for use on a VAX computer.

V. SIMULATION RESULTS

The theory developed in the previous sections is use to model the disturbances produced by the release of H_2O, and CH_3OH into the ionosphere. The ambient O^+ and H^+ densities are 10^6 and 10^3 cm^{-3}, respectively. The simulation considers the release of 10^{26} molecules (a few kilograms) of each species at 300 km altitude. The neutral composition at that altitude is given in Table V. The computed diffusion coefficients are 3.4×10^{10}, and 1.0×10^{10} cm^2/s for water vapor and methyl alcohol, respectively. The release is assumed to occur at night so that solar illumination does not affect the chemistry.

Table V

Temperature and Concentrations of

Neutral Species at 300 km Altitude

T	990 K
[O]	6.2×10^8 cm^{-3}
$[O_2)$	4.7×10^6 cm^{-3}
$[N_2]$	1.3×10^8 cm^{-3}
[He]	3.7×10^6 cm^{-3}
[H]	1.7×10^5 cm^{-3}

The major uncertainty is the branching ratios for production of excited vibrational states. For this simulation, we have assumed that all allowed vibrational levels are equally populated. For example, all 10 vibrational states of $OH(X^2\Pi_i, v=0,1,2,\ldots,9)$ in reaction (19) are taken to be generated with probability equal to 1/10. These states will also be generated by cascading from higher energy electronic or vibrational states. The branching ratios are parameters which can be adjusted according to

future theoretical and experimental considerations. It should also be noted that rotational splitting of the lines has been neglected. This can readily be added for a given rotational temperature.

Figures 1 through 6 show the computed composition out to radius of 19 km from the center of the release after 128 seconds. The radial profiles of the background atomic ions show a depression within 4 kilometers of the release (Figure 1). The molecular ions (OH^+, H_2O^+, and H_3O^+) from the water interactions fill in the void produced by depletion of the atomic (O^+ and H^+) ions. Dissociative recombination of the molecular ions (H_2O^+ and H_3O^+) is the primary source for the vibrationally excited OH shown in Figure 2. The metastable states of atomic oxygen are present only because they have long lifetimes. The intensities from metastables are much lower than the intensities from the molecular species. The primary source for vibrationally excited water is reaction (39) of atomic oxygen with methyl alcohol. Only 10% of the $H_2O(v)$ comes from the dissociative recombination reaction (25) which can be traced back to the water release. The final product of the H_2O release are debris neutrals which are dominated by H_2O, H, and O (Figure 3). The final abundance of OH is relatively low because of its high reactivity.

Seven organic molecular ions are produced as a result of interactions with the methyl alcohol vapors (Figure 4). Each one of these is a potential source of a radiation through dissociative recombination reactions. As shown in Figure 5, the two dominant infrared emitters will be vibrationally excited formaldehyde (CH_2O) and dimethyl ether (CH_3OCH_3). The primary sources for $CH_2O(v)$ are ion-molecule reaction (18), dissociative recombination reaction (30) and neutral reaction (39). It is likely that any of the eight organic species shown in Figure 6 will also contribute to the emission spectra.

A time history of the airglow from the vibrational, electronic and vibronic states of several species is summarized in Figure 7. The sum of the intensities from all excited states of each molecule plotted as a function of time after release. The superscript * and the (v) designate vibronic and vibrational excitation, respectively. Most of the emissions peak within a few seconds after release. The metastable states of oxygen produce emissions peak much later. OH(v), $H_2O(v)$, and $CH_2O(v)$ are the strongest infrared emitters. The most strongly excited of the vibronic species will be OH^* which is produced by reactions (24) and (25). The emissions from vibronic states of water are relatively weak because of the low percent of H_2O^* produced by dissociative recombination of H_3O^+.

Emissions from the metastable states of oxygen are the strongest lines produced by CO_2 releases in the ionosphere [Bernhardt, 1987]. The emissions from $O(^1D)$ and $O(^1S)$ are relatively weak for H_2O and CH_3OH releases because there is no direct process to excite them.

The spectra from excited OH covers 240 nm to 4400 nm wavelengths. The near ultraviolet spectrum from the $OH(A^2\Sigma^+)$ is computed for four seconds after release to give the intensities in Figure 8a. The intensities of around 1 kR are consistent with measurements made by a rocket borne photometer at 306.4 nm during the Waterhole I experiment [Yau et al., 1985] when H_2O was explosively deposited into the auroral ionosphere. Our computations show that the emissions from vibrational OH will be substantially stronger.

The vibrational spectrum for chemically induced Meinel bands of OH show intensities between 1-R and 3×10^4-R. The visible emissions four seconds after release are relatively weak (Figure 8b) because the vibrational transitions with Δv of 4 or 5 are not fed by cascading from vibronically excited states and the transition probabilities are low. The

strongest emissions (Figures 8c and d) result from low lying vibrational levels from small values of Δv.

After 128 seconds, the intensities of the emissions lines has been reduced but the levels are still significant. The near ultraviolet intensities are 40-R or lower (Figure 9a) and the Meinel band intensities (Figures 9b,c and d) are reduced by a factor of thirty below the corresponding values at t = 4 seconds.

VI. Conclusions

The chemical interactions of a single molecular species with the plasma constituents of the upper atmosphere can generate a large number of new, excited species. An H_2O release by itself yields vibrational states of H_3O^+, H_2O^+, OH^+, OH, and H_2O along with electronic states of OH and O. Several sources of energy are available to excite the molecules including chemical energy from reactions, kinetic energy from the gas injection, solar energy and energy from collisions by electrons. This study has concentrated on ion-molecule and neutral-molecule chemistry as the source of excitation energy. With these sources, we find that a wide range of light emissions can be stimulated by a single H_2O release. Intensities of 1 kR or more can be generated between 240 nm and 4400 nm wavelengths.

The addition of CH_3OH to the release produces many new excited species of the form $C_aH_bO_c$ where a, b, and c are small integers. Enhanced vibrational emissions from OH(v) are produced by the release of either species. Emissions from CH_2O are uniquely identified with the CH_3OH release but the addition of water enhances the formation of vibrational formaldehyde via reaction (18). The example considered here demonstrates that the interaction of gases in a mixture may enhance the emissions from selected species (ie., CH_2O).

For releases at 300 km altitude, the airglow emissions from chemical reactions may have equal contributions from neutral-neutral reactions, ion-neutral reactions, and electron-ion reactions. The emission chemistry for releases much below this altitude will probably be dominated by neutral-neutral reactions because of the increase in the background neutral densities. Releases above this altitude will be affected primarily by reactions with the ambient plasma. At 300 km or above, the loss of excited states is primarily by radiation. At much lower altitudes, quenching of excited states by reactions with neutrals may be important.

Finally, our test case has led us to postulate that the emissions from molecules released into the nighttime F-layer will come from fragments of the parent molecule or from excited atomic oxygen. The H_2O and CH_3OH releases studied here yield enhance OH and CH_2O emissions, respectively. For similar species, the emissions will come from radicals produced by detaching hydrogen from the released molecule.

The next logical step for this study is to make optical observations of H_2O and other releases which occur in the night ionosphere. Ground based spectrographs can be employed to record the wide range of emissions which we have predicted. The observations should be made under different conditions of solar illumination, at different altitudes, and at different injection velocities to separate the effects of the different energy sources described above. Such experiments have been proposed by us for future Space Shuttle missions.

ACKNOWLEDGMENTS

This research has been sponsored by the Lockheed Missiles and Space Company.

VII. REFERENCES

Albritton, D. L., Ion-neutral reaction-rate constants measured in flow reactors through 1977, At. Data Nucl. Data Tables, 22, 1, 1978.

Anderson, D. A., and P. A. Bernhardt, Modeling the effects of an H_2 gas release on the equatorial ionosphere, J. Geophys. Res., 83, 4777, 1978.

Bernhardt, P. A., Three-dimensional, time-dependent modeling of neutral gas diffusion in a nonuniform, chemically reactive atmosphere, J. Geophys. Res., 84, 793, 1979.

Bernhardt, P. A., A critical comparison of ionospheric depletion chemicals, J. Geophys. Res., 92, 4617-4628, 1987.

Bernhardt, P. A., Cross-B convection of artificially created, negative-ion clouds and plasma depressions: Low-speed flow, J. Geophys. Res., 93, 8696-8704, 1988a.

Crosley, D. R., and R. K. Lengel, Relative transition probabilities and the electronic transition moment in the A-X system of OH, J. Quant. Spectrosc. Radiat. Transfer., 15, 579-591, 1975.

Fraser, M. E., A. Gelb, B. D. Green, Calculation of space station infrared irradiance form atmosphere-induced emissions, A Study of Space Station Contamination Effects, NASA Conference Publication 3002, 1988.

Herbst, E., What are the products of polyatomic ion-electron dissociative recombination reactions, Ap. J., 222, 508-516, 1978.

Ikezoe, Y. S. Matsuoka, T. Masahiro, A. Viggiano, Gas phase ion-molecule reaction rate constants through 1986, Maruzen Co., Ltd., Tokyo, 1987.

Kondratiev, V. N., Rate Constants of Gas Phase Reactions, National Bureau of Standards, Washington, DC, January 1972.

Lew, H., Electronic spectrum of H_2O^+, Can. J. Phys., 54, 2028-2049, 1976.

Llewellyn, E. J., B. H. Long and B. H. Solheim, The quenching of OH^* in the atmosphere, Planet. Space Sci., 26, 525-531, 1978.

McDade, L. C., and E. J. Llewellyn, Mesospheric oxygen and atom densities inferred from night-time OH Meinel band emission rates, Planet. Space Sci., 36, 897-905, 1988.

Mies, F. H., Calculated vibrational transition probabilities of $OH(X^2\Pi)$, J. Mole. Spect., 53, 150-188, 1974.

Mitchell, J. B. A., and J. W. McGowan, Experimental studies of electron-ion recombination, in Physics of Ion-Ion and Electron-Ion Collisions, edited by F. Brouillard and J. W. McGowan, Plenum, New York, 1983.

Rowe, B. R., F. Vallee, J. L. Queffelec, J. C. Gomet, and J. Mortais, The yield of oxygen and hydrogen atoms through dissociative recombination of H_2O^+ ions with electrons, J. Chem. Phys., 88, 845-850, 1988.

Schofield, K., An evaluation of kinetic rate data for reactions of neutrals of atmospheric interest Planet. space Sci., 15, 643-670, 1967.

Wang, H. T., W. S. Felps, and S. P. McGlynn, Molecular Rydberg States. VII. Water, J. Chem. Phys., 67, 2614-2628, 1977.

Yau, A. W., B. A. Whalen, F. R. Harris, R. L. Gattinger, M. B. Pongratz, and P. A. Bernhardt, Simulations and observations of plasma depletion, ion composition, and airglow emissions in two auroral ionospheric depletion experiments, J. Geophys. Res., 90, 8387, 1985.

Zipf, E. C., The dissociative recombination of O_2^+ ions into specifically identified final atomic states, Bull. Amer. Phys. Soc., 15, 418, 1970.

Zipf, E. C., A laboratory study on the dissociative recombination of vibrationally excited O_2^+ ions, J. Geophys. Res., 85, 4232-4236, 1980.

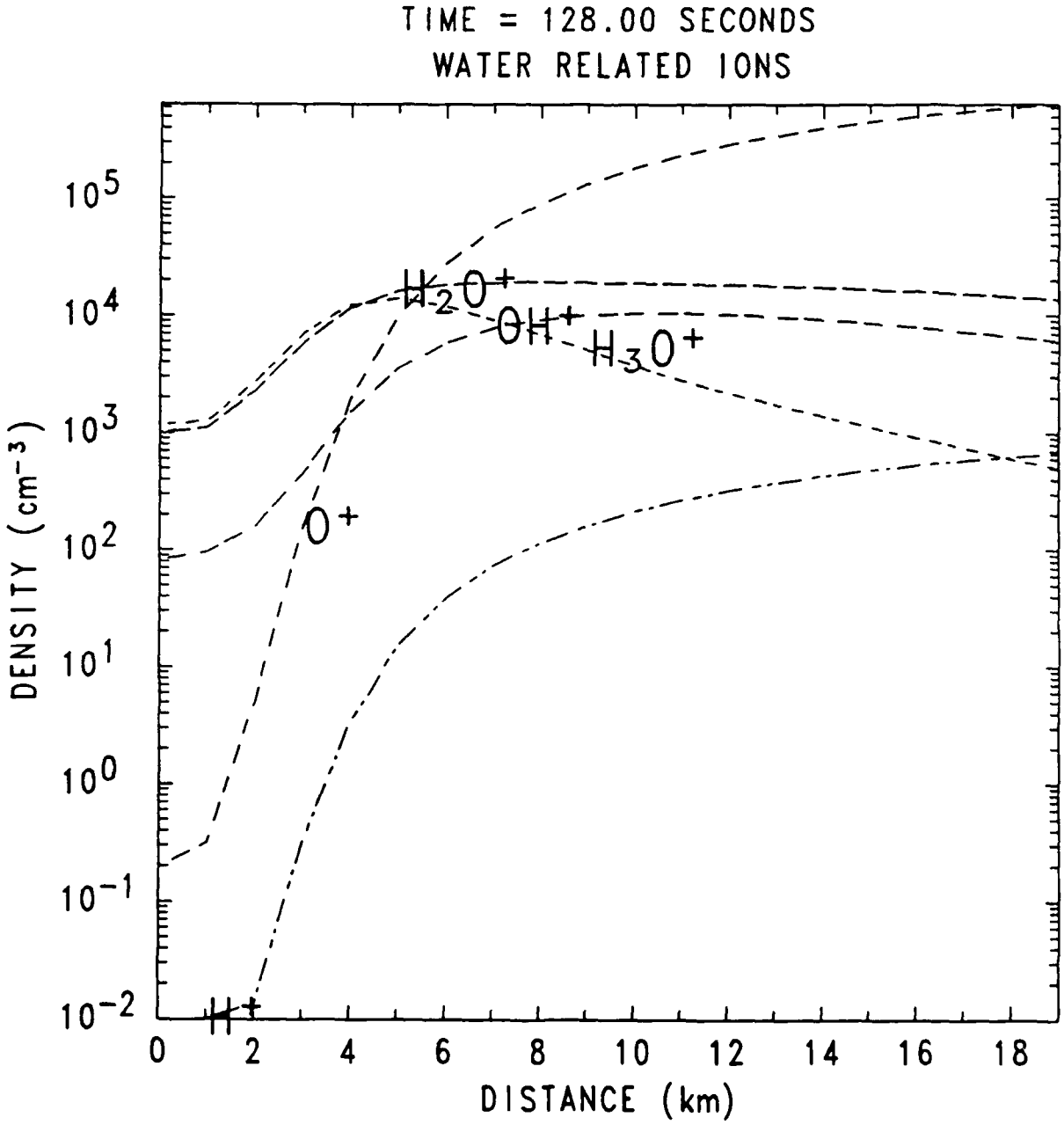

Figure 1. Radial profiles of OH_n^+ ions (n=0,1,2,3) in the modified ionosphere 128 seconds after the release of 10^{26} molecules each of H_2O and CH_3OH. The hydroxyl, water and hydronium ions are directly produced by the water component of the release.

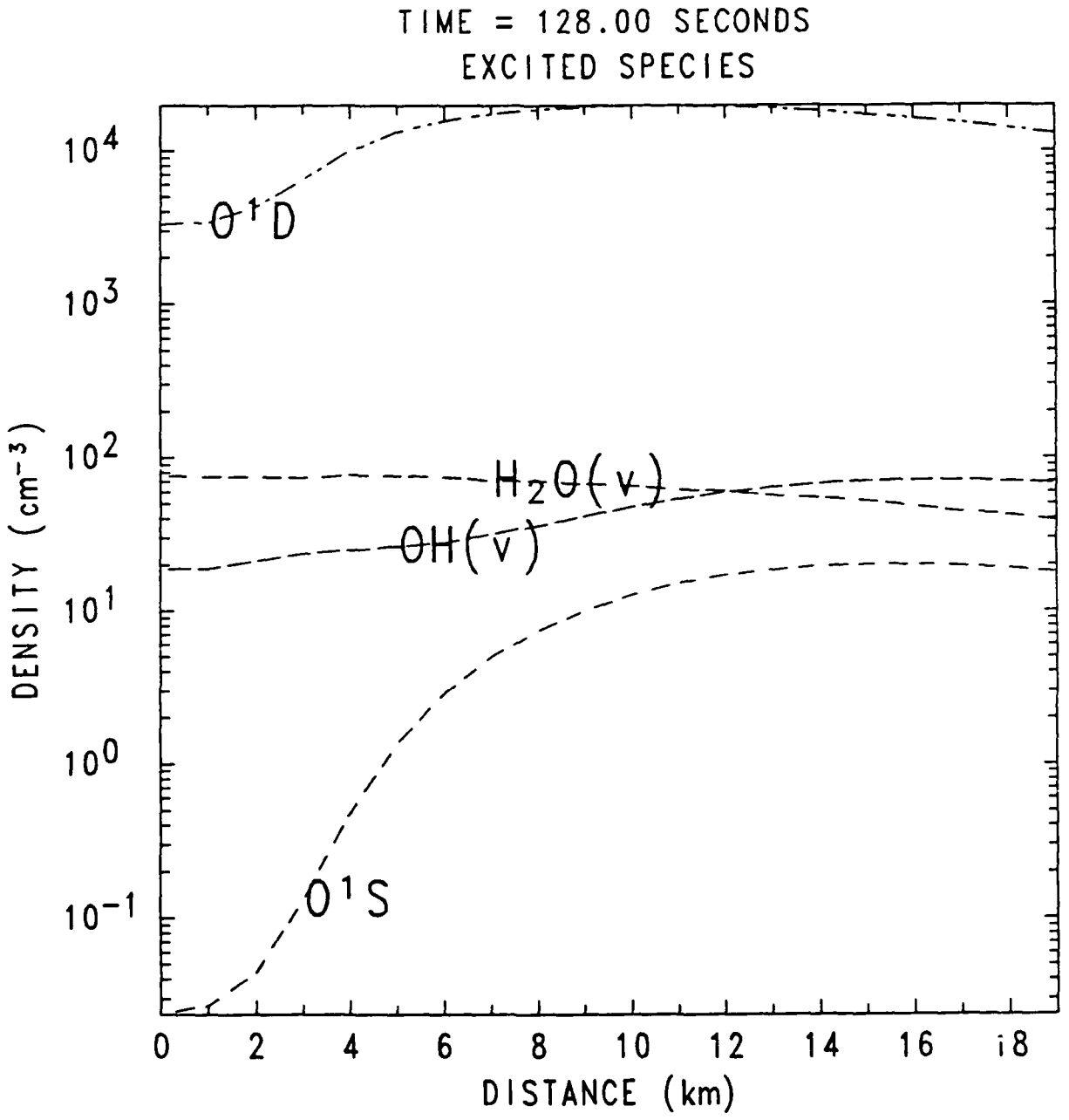

Figure 2. Excited species with the form OH_n (n=1,2,3) resulting from dissociative recombination of electrons with the molecular ions found in Figure 1. Vibronic states of OH and H_2O are not shown.

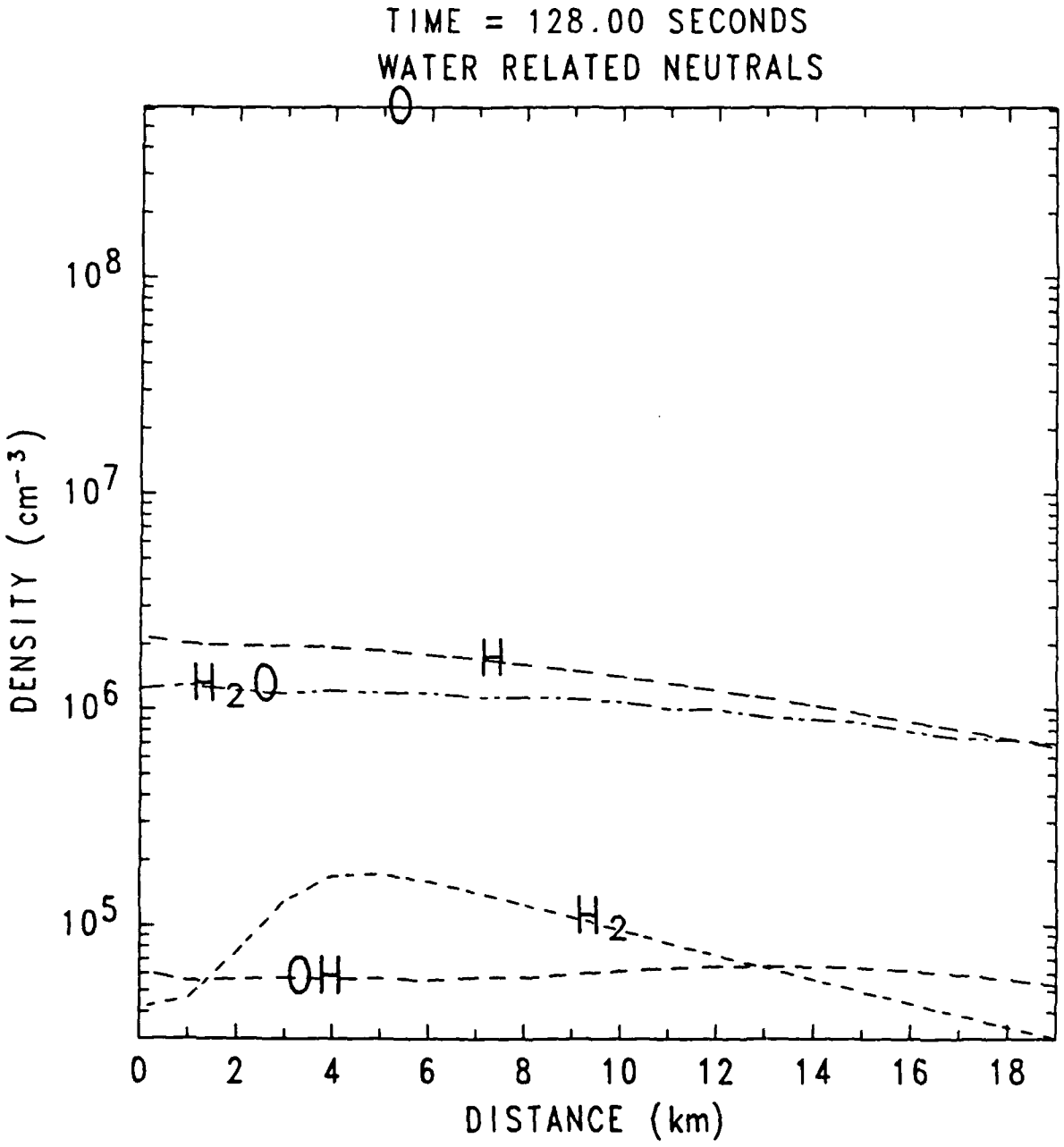

Figure 3. Enhanced concentrations of neutrals resulting from the water component of the release.

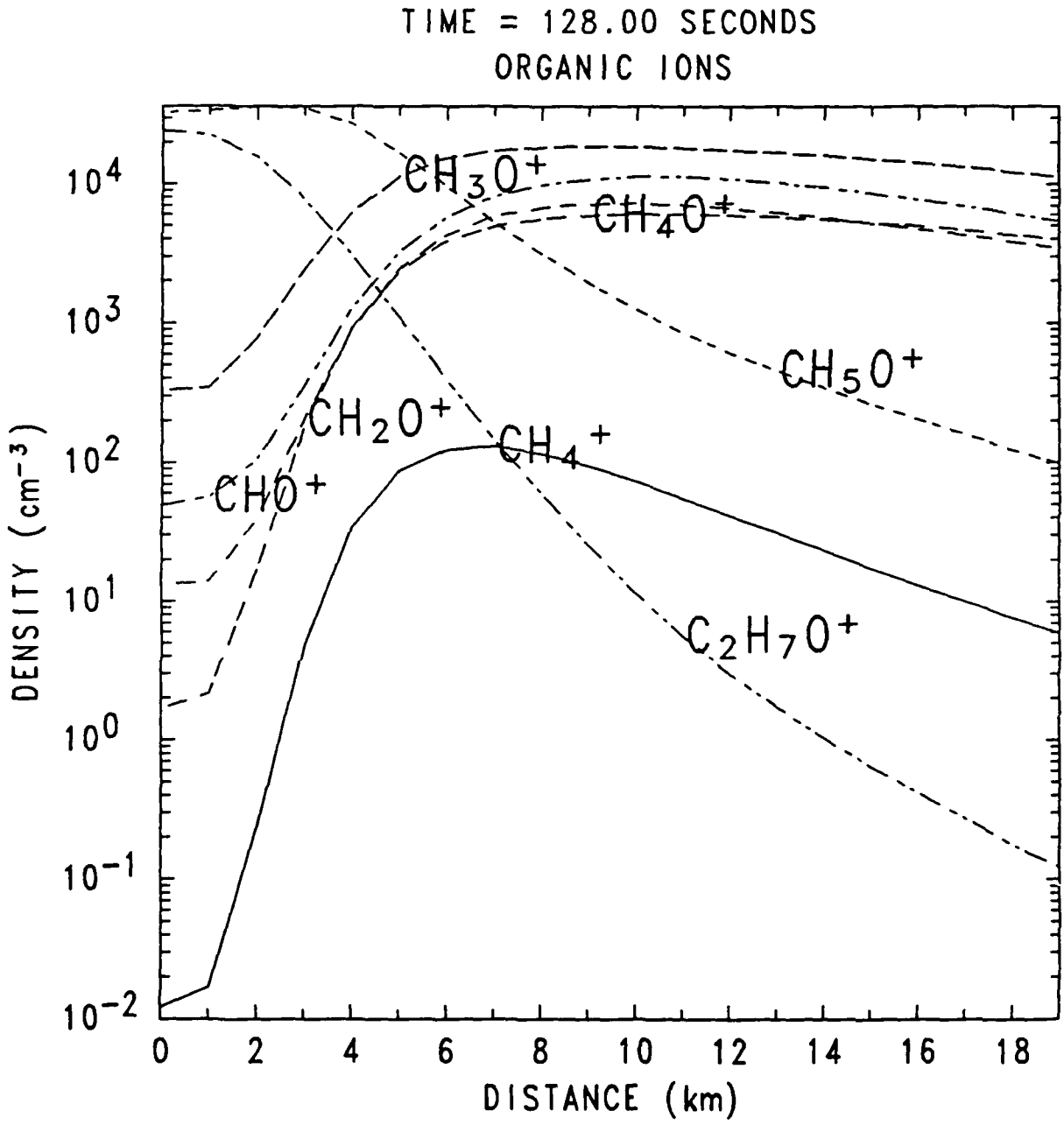

Figure 4. Radial profiles of CH_nO^+ (n=1,2,3,4,5), $H^+ \cdot CH_3OCH_3$, and CH_4^+ ions produced by ion molecule reactions triggered by the CH_3OH component of the release.

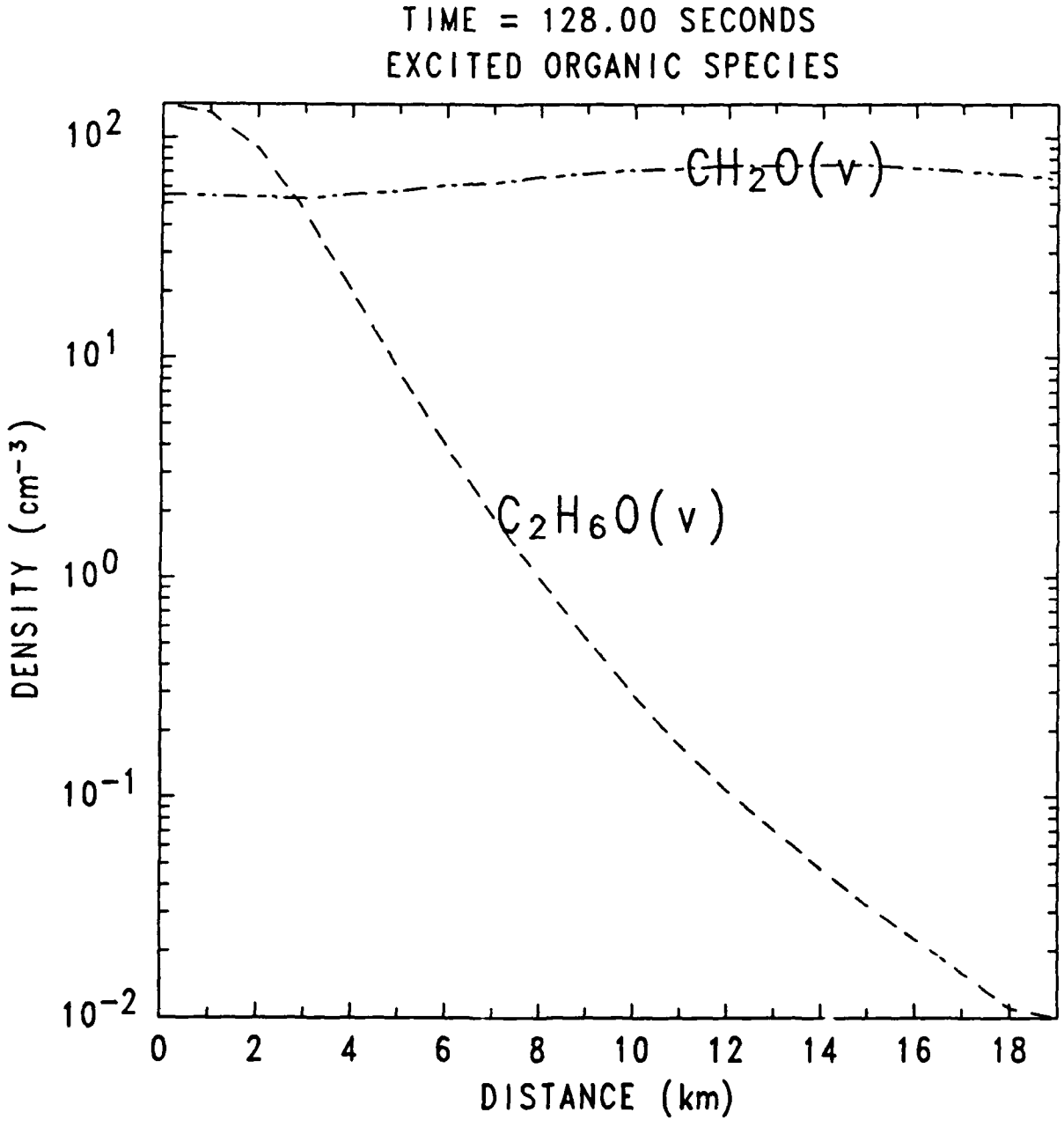

Figure 5. Vibrationally excited organic molecules produced by the methyl alcohol release.

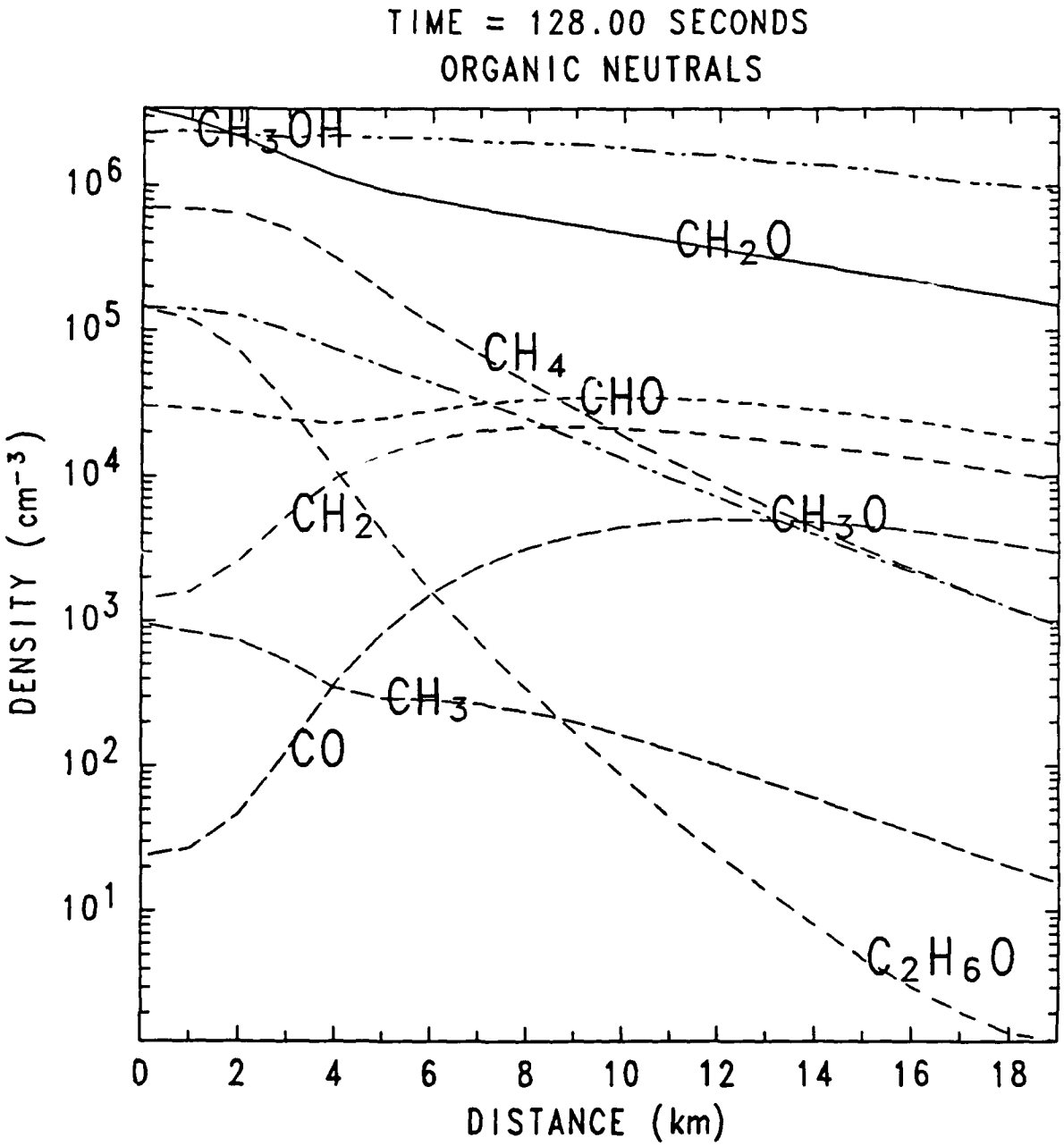

Figure 6. Artificially created concentrations of neutral molecules of the form CH_n (n=2,3,4), CH_nO (n=0,1,2,3,4), and CH_3OCH_3.

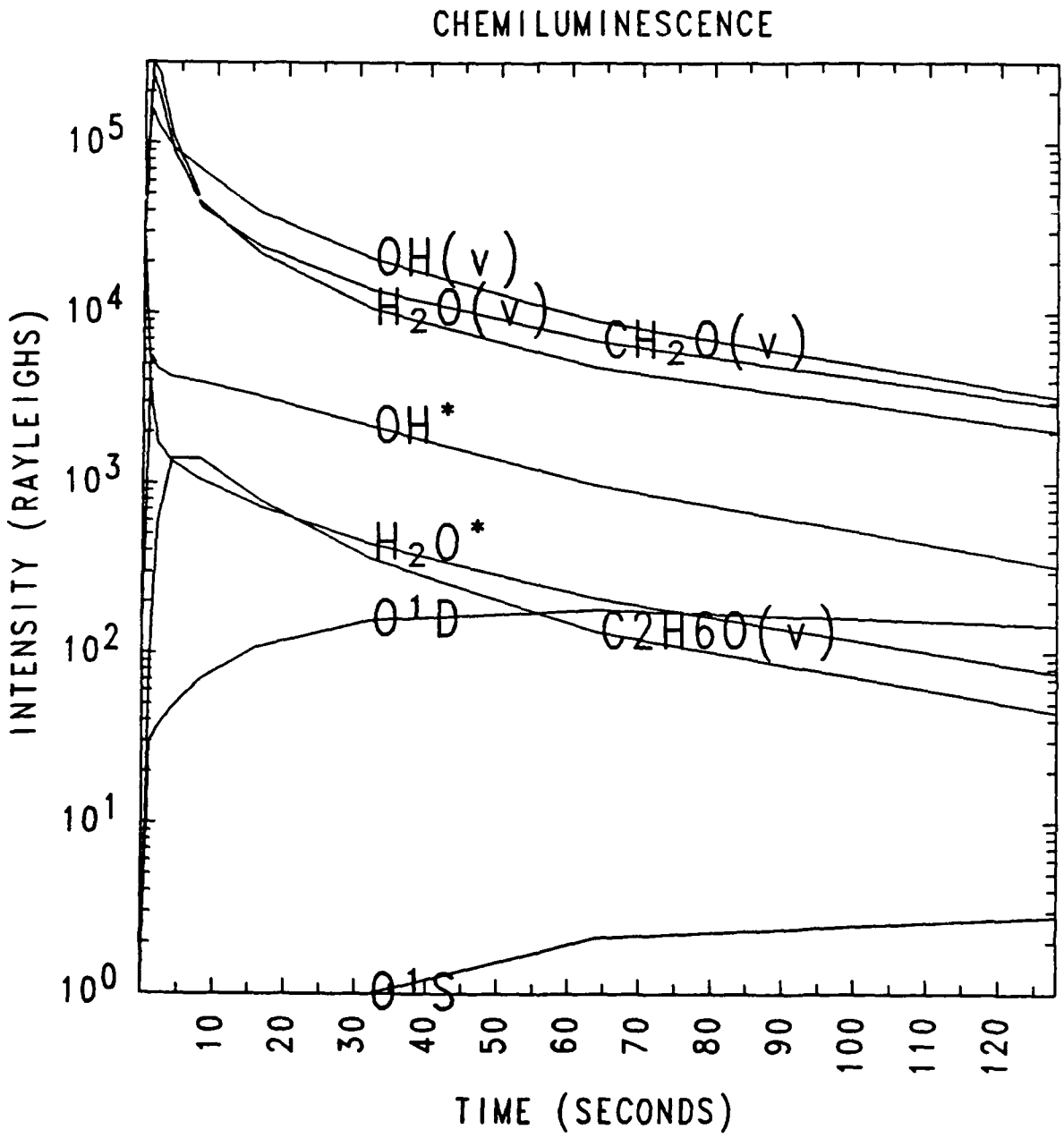

Figure 7. Variations in the light intensities from vibrational and vibronic states. Ion-molecule and electron-ion reactions between the ionosphere and the released gases provide the excitation energy.

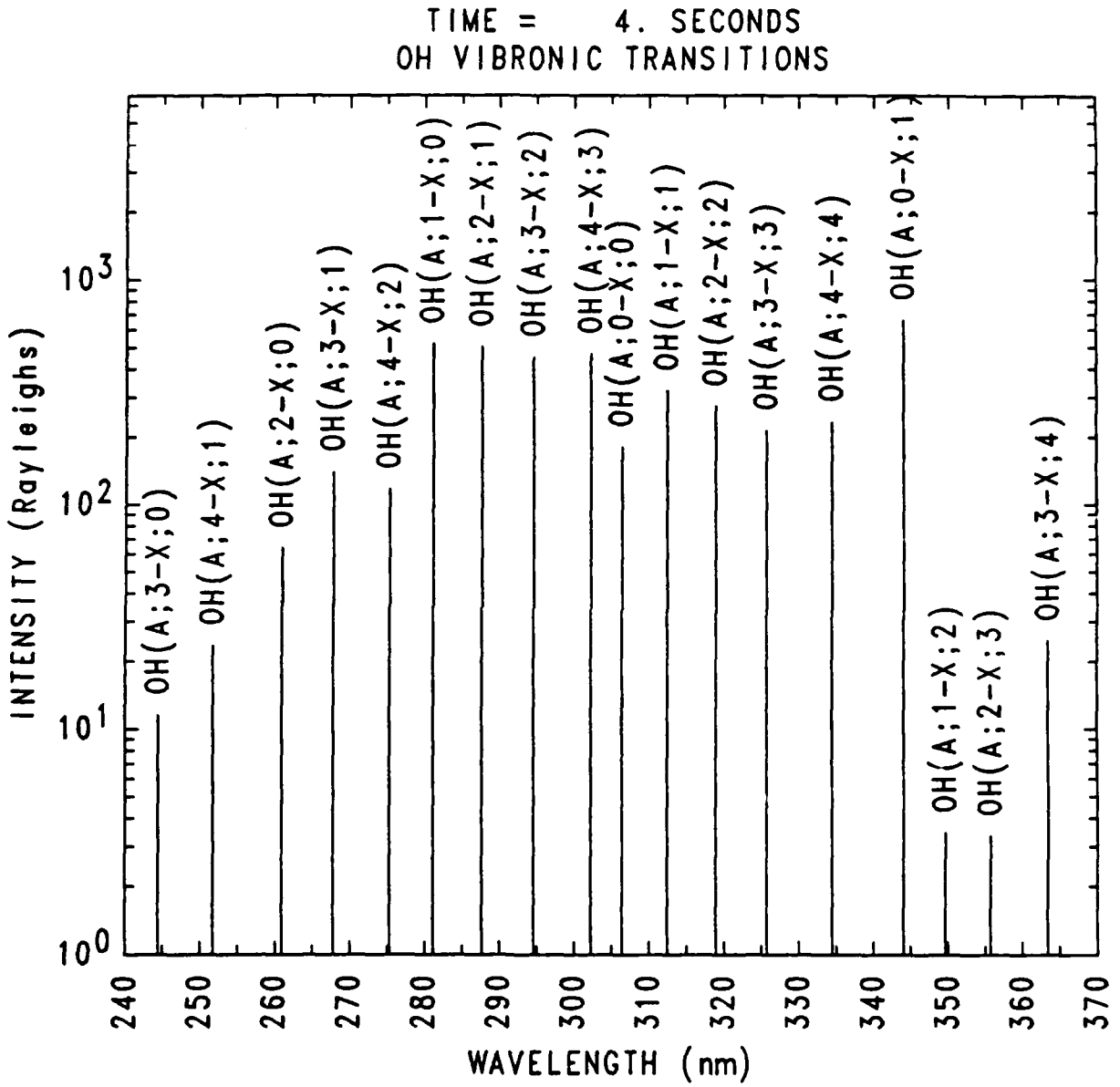

Figure 8a. Computed intensities of near ultraviolet emissions from $OH(A^2\Sigma^+;v') \rightarrow OH(X^2\Pi_i,v'')$ transitions, four seconds after the release.

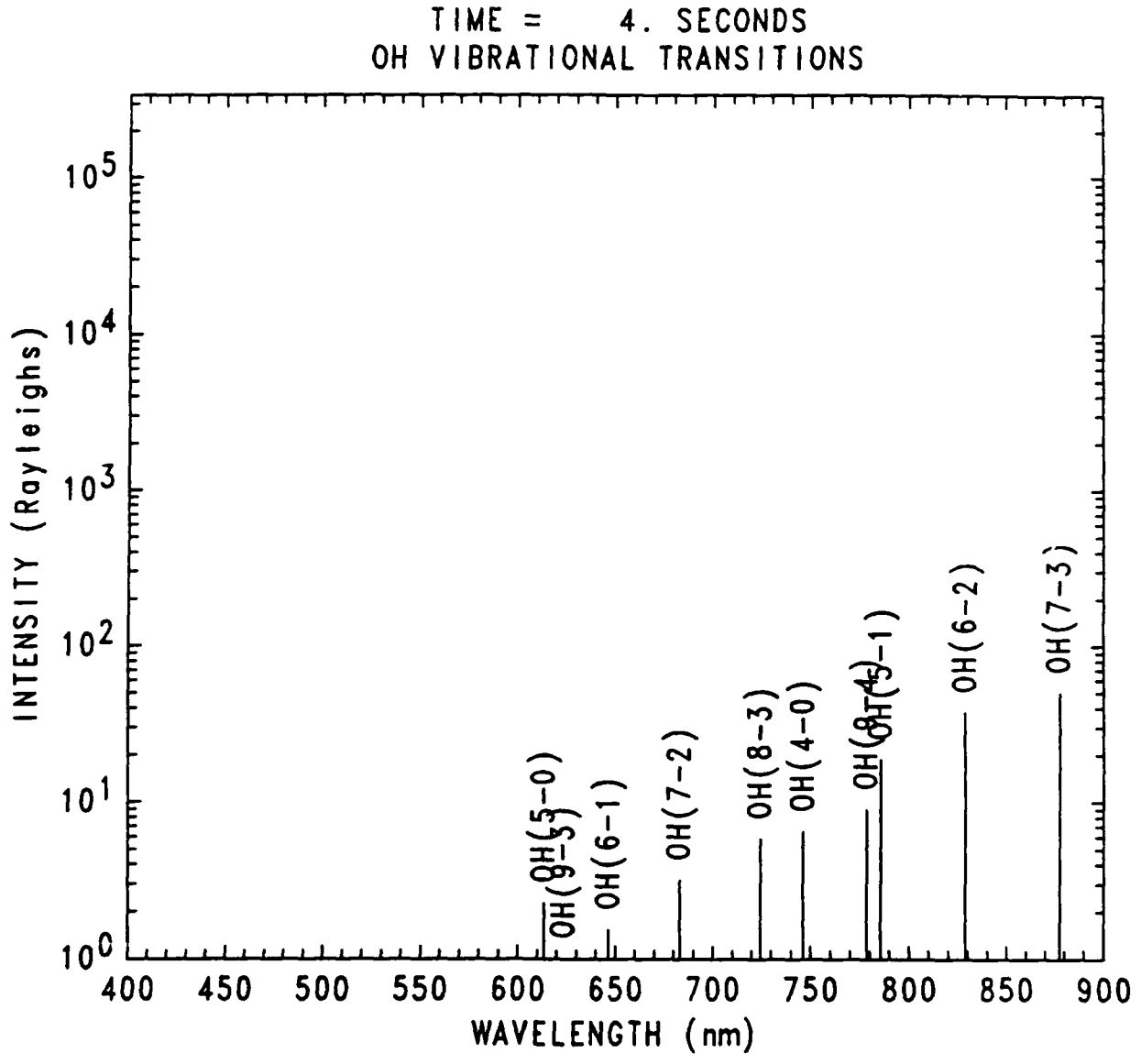

Figure 8b. Computed intensities of visible emissions from vibrational $OH(X^2\Pi_i;v'\rightarrow v'')$ transitions, four seconds after the release.

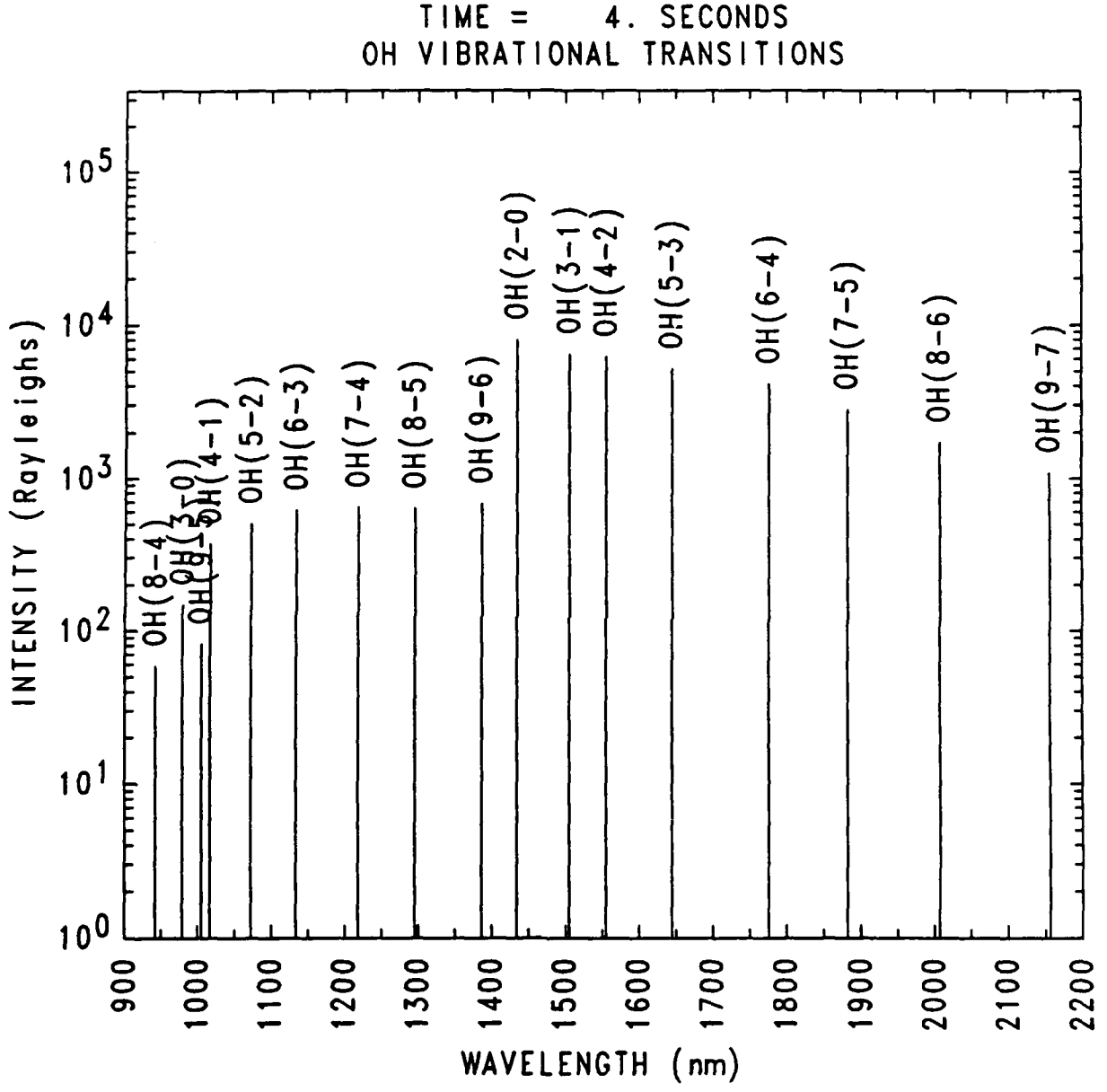

Figure 8c. Computed intensities of near infrared emissions from vibrational transitions of OH, four seconds after the release.

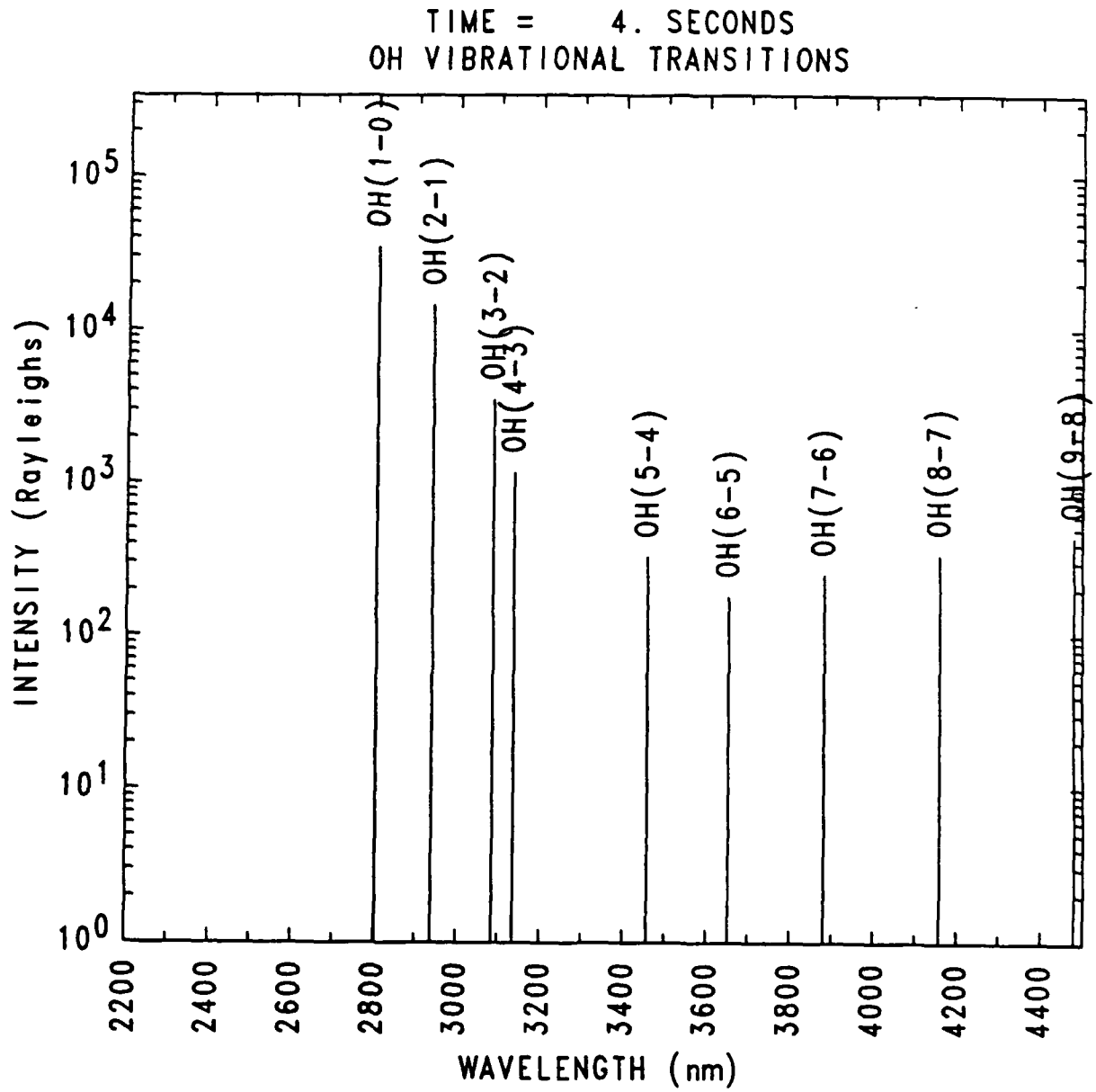

Figure 8d. Computed intensities of infrared emissions from vibrational transitions of OH, four seconds after the release.

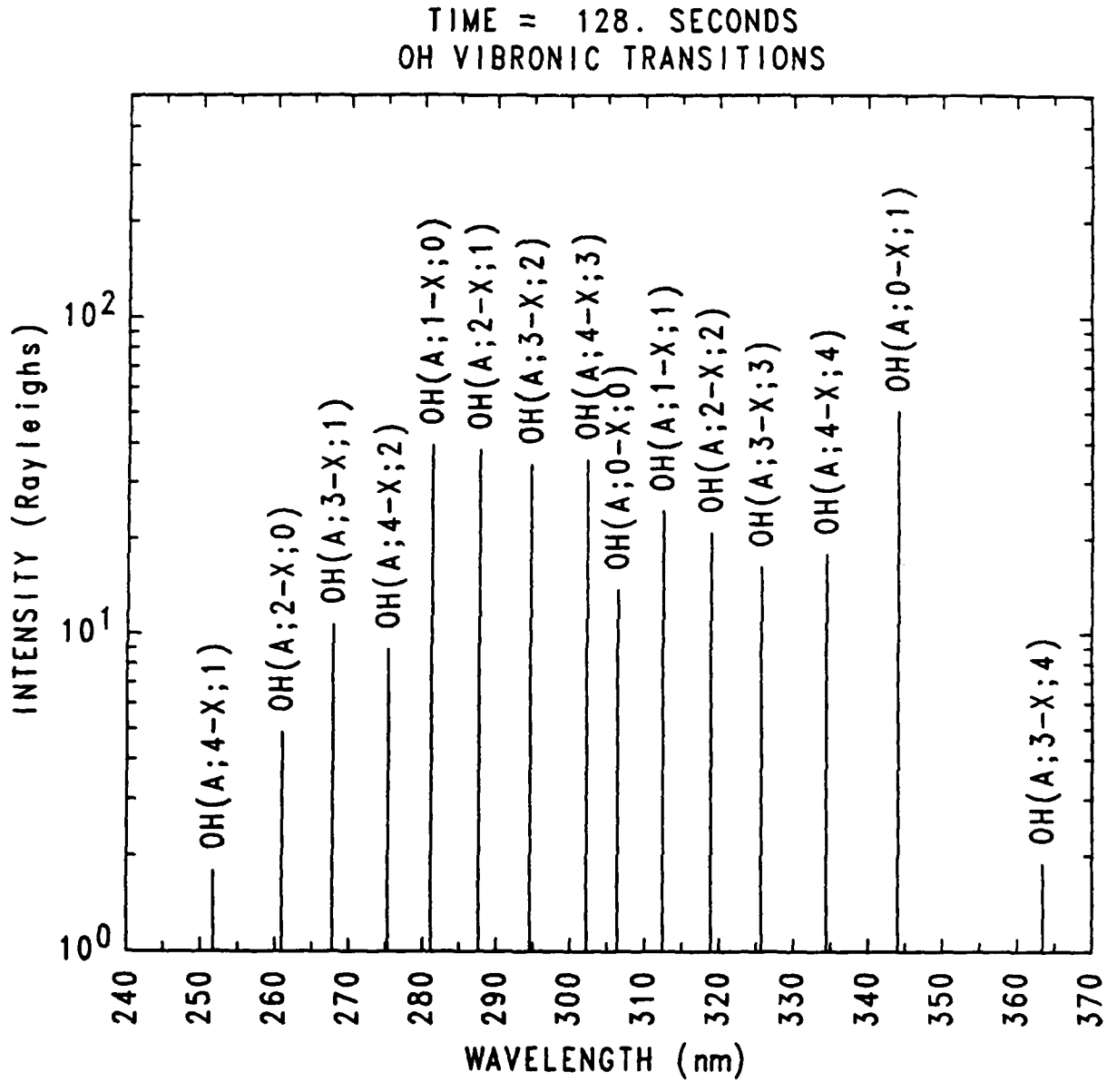

Figure 9a. Computed intensities of near ultraviolet emissions from $OH(A^2\Sigma^+;v') \rightarrow OH(X^2\Pi_i,v")$ transitions, 128 seconds after the release.

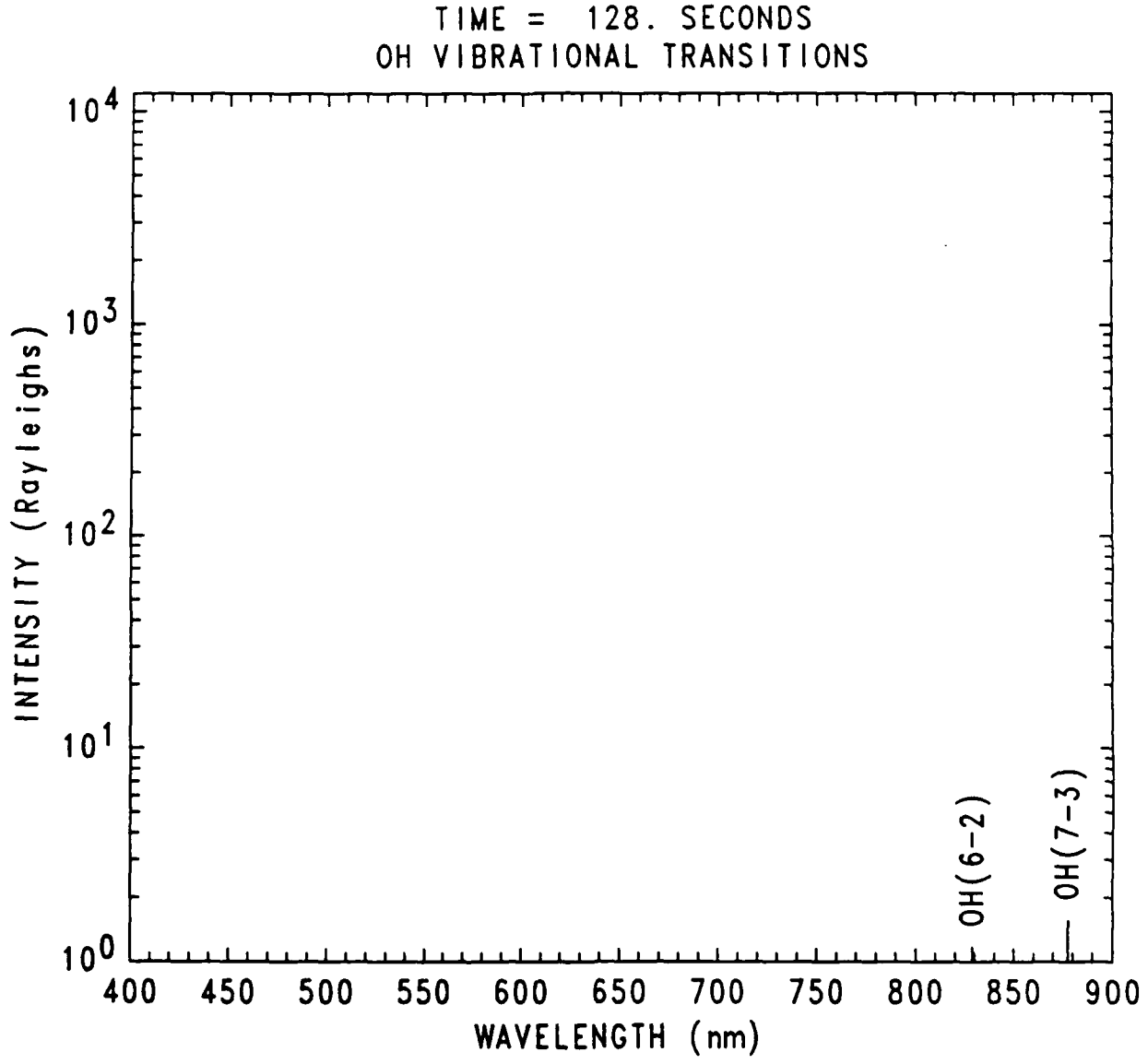

Figure 9b. Computed intensities of visible emissions from vibrational $OH(X^2\Pi_i; v' \rightarrow v'')$ transitions, 128 seconds after the release.

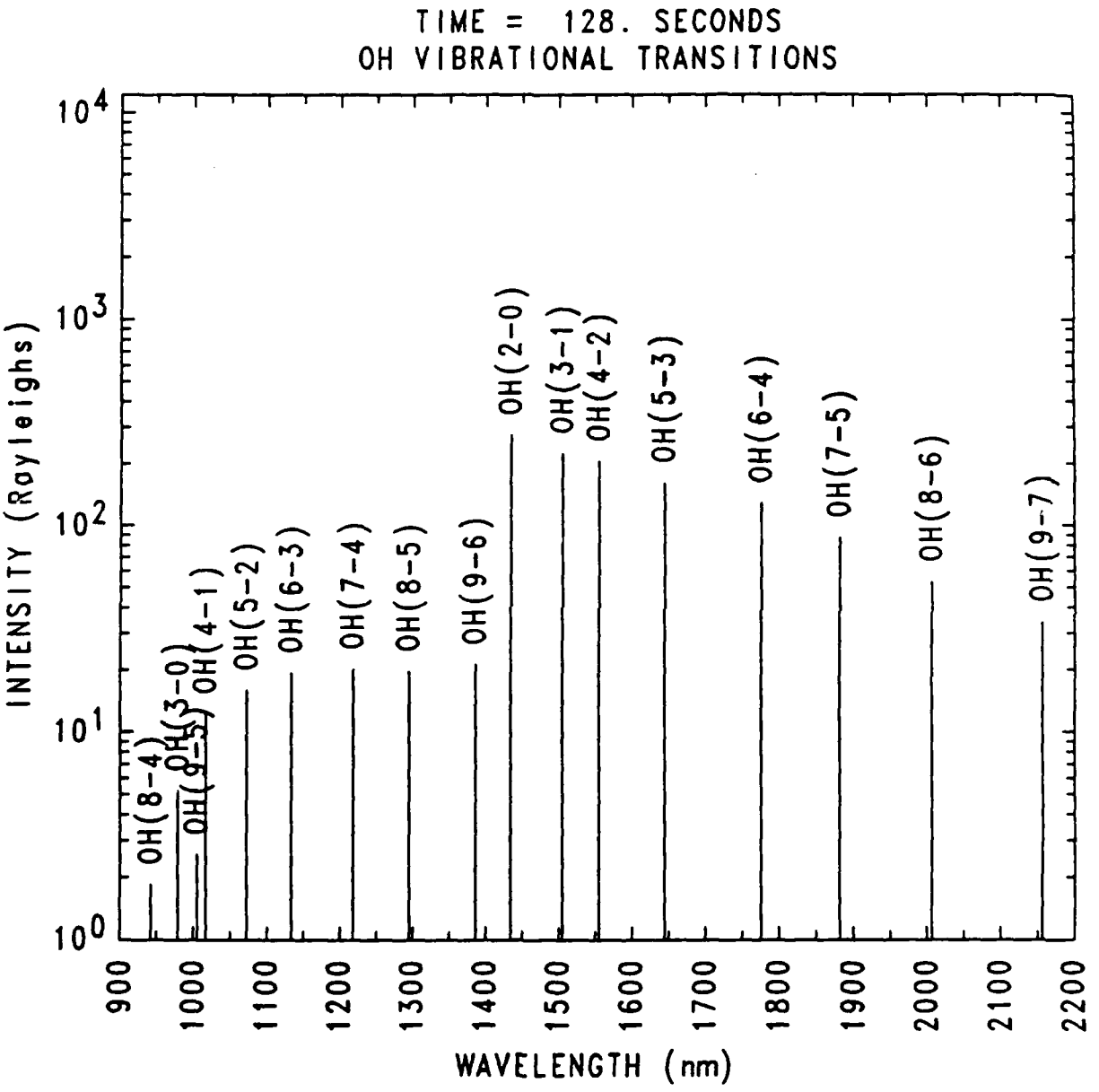

Figure 9c. Computed intensities of near infrared emissions from vibrational transitions of OH, 128 seconds after the release.

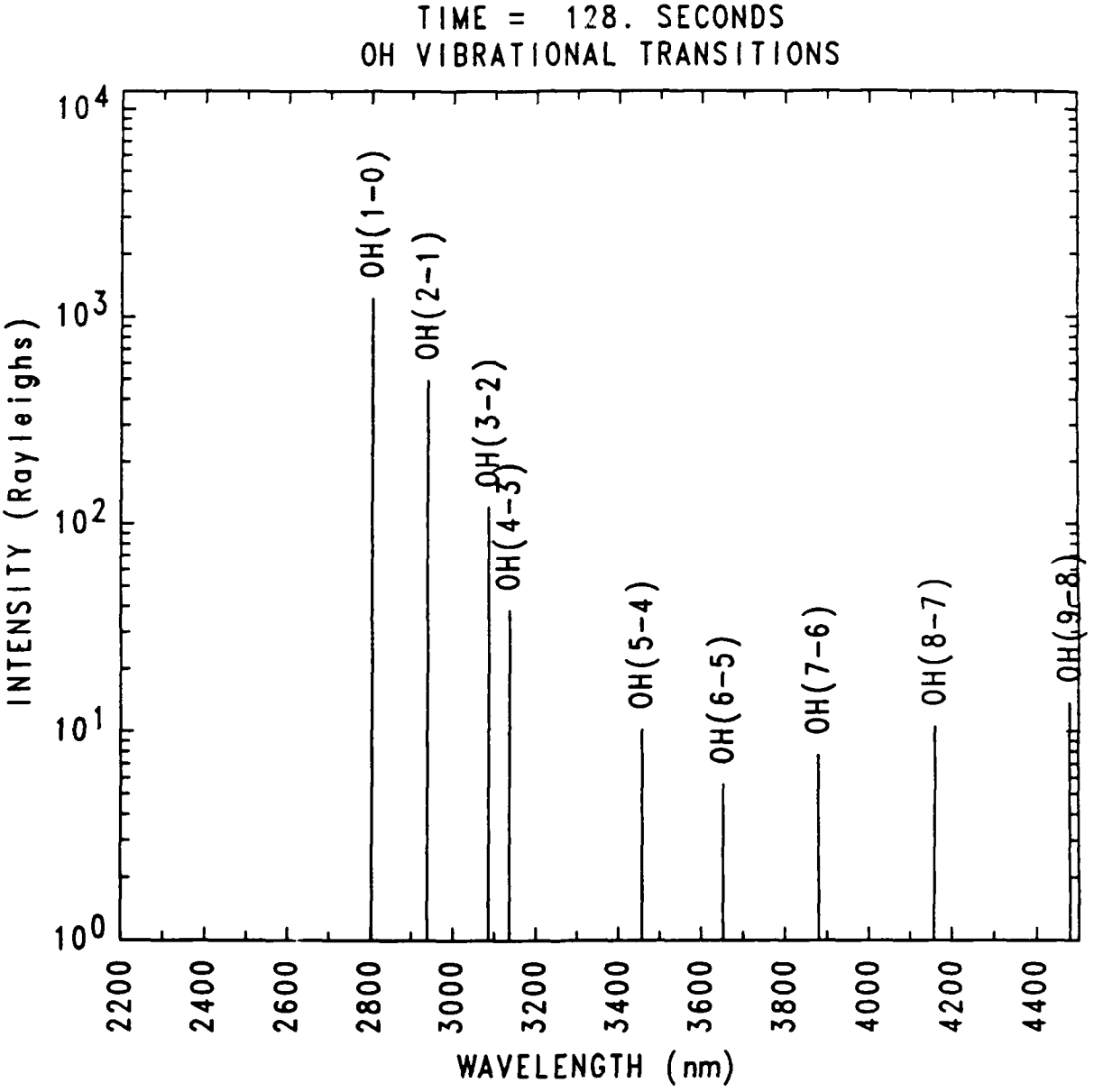

Figure 9d. Computed intensities of infrared emissions from vibrational transitions of OH, 128 seconds after the release.

DISTRIBUTION LIST
(UNCLASSIFIED ONLY)

PLEASE DISTRIBUTE ONE COPY TO EACH OF THE FOLLOWING PEOPLE (UNLESS OTHERWISE NOTED)

Director
Naval Research Laboratory
Washington, DC 20375-5000
Code 4100
Code 4700 (26 copies)
Code 4701
Code 4780 (30 copies)

F.O. von Bun
Code E
National Aeronautics and
Space Administration
Washington, DC 20546

G.S. Arnold
Chemistry and Physics Laboratory
The Aerospace Corporation
P.O. Box 95957
Los Angeles, CA 90009

G.E. Caledonia
Physical Sciences, Inc.
Dascomb Research Park
P.O. Box 3100
Andover, MA 01810

J.T. Dickinson
Department of Physics
Washington State University
Pullman, WA 99164-2814

B.D. Green
Physical Sciences, Inc.
Dascomb Research Park
P.O. Box 3100
Andover, MA 01810

D.F. Hall
Chemistry and Physics Laboratory
The Aerospace Corporation
P.O. Box 92957
Los Angeles, CA 90009

C.E. Keffer
Center for Space Plasma and Aeronomic
Research
The University of Alabama in
Huntsville
Huntsville, AL 35899

J.L. Leger
Code ES5
NASA/Johnson Space Center
Houston, TX 77058

E.R. Miller
Code ES61
NASA/Marshall Space Flight Center
Huntsville, AL 35812

R.O. Rantanen
Science and Engineering Assoc., Inc.
6535 S. Dayton Street, Suite 2100
Englewood, CO 80111

W.R. Seebaugh
Science and Engineering Assoc., Inc.
6535 S. Dayton Street
Englewood, CO 80111

N. Singh
Department of Electrical and Computer
Engineering
The University of Alabama in
Huntsville
Huntsville, AL 35899

J.F. Spann
Code ES55
NASA/Marshall Space Flight Center
Huntsville, AL 35812

Arnold Barnes
ANSER Suite 800
1215 Jefferson Davis Hwy.
Arlington, VA 22202

Peter F. Bythrow
The Johns Hopkins University
Applied Physics Laboratory
Johns Hopkins Road
Laurel, MD 20707

James Carbary
The Johns Hopkins University
Applied Physics Laboratory
Johns Hopkins Road
Laurel, MD 20707

David Dimiduk
Directed Energy Office
SDIO, The Pentagon
Washington, DC 20301-7100

Fred Finlayson
The Aerospace Corp. M7 633
PO Box 92957
Los Angeles, CA 90009-2957

John A. Fleming
Ball Space Systems
PO Box 1062
Boulder, CO 80306

Paul H. Geithner
USAF/HQ Space Div./CNIS
PO Box 92960
Los Angles, CA 90009-2960

Robert E. Gold
The Johns Hopkins University
Applied Physics Laboratory
Johns Hopkins Road
Laurel, MD 20707

Michael Griffin
SDIO, The Pentagon
Washington, DC 20301-7100

Frank Grose
Applied Research Inc.
PO Box 11220
Huntsville, AL 32814-1220

Richard Gullickson
SDIO/CS
The Pentagon
Washington, DC 20301-7100

Thomas Hayhurst
The Aerospace Corp.
M/S M2/251
PO Box 92957
Los Angeles, CA 90009-2957

Ronald Herm
The Aerospace Corp.
PO Box 92957
Los Angeles, CA 90009

Glen Hohnstreiter
Sandia National Laboratories
Org. 9142
Albuquerque, NM 87185-5800

Arnold Kramish
Systems Planning
(SDIO)
Washington, DC 20301-7100

Owen Lewis
Photon Research Association
1911 N. Fort Myer Drive
Suite 408
Arlington, VA 22209

William Arthur Millard
Sandia National Laboratories
Div. 1555
Albuquerque, NM 87185-5800

Dr. John Morris
Applied Research Inc.
5025 Bradford Blvd.
PO Box 11220
Huntsville, AL 35814-11220

Dr. Randall Murphy
AFGL
GL/OP
HAFB Bradford, MA 01731

Thomas L. Roche
The Johns Hopkins University
Applied Physics Laboratory
Johns Hopkins Road
Laurel, MD 20707

Maxwell Sanford
Los Alamos Natl. Lab
PO Box 1663 M/S B232
Los Alamos, NM 87545

Ronald Saxon
The Johns Hopkins University
Applied Physics Laboratory
Johns Hopkins Road
Laurel, MD 20707

Dominic J. Scrooc
The Aerospace Corp.
P.O. Box 92957
Los Angeles, CA 90009

Frederick S. Simmons
The Aerospace Corp.
P.O. Box 92957 M1/126
Los Angeles, CA 90009

Robert Suggs
Applied Research Inc.
5025 Bradford Blvd.
Huntsville, AL 35803

Tushar Suthar
ANSER, Suite 800
1215 Jefferson Davis Hwy.
Arlington, VA 22202

Major Steve Theriault
SDIO
Pentagon
Washington, DC 20301-7100

Kyle Zeringue
Applied Research Inc.
5025 Bradford Blvd.
Huntsville, AL 35805

Richard Verga
OSD/SDIO/T/KT
The Pentagon
Washington, DC 20301-7100

LTC Mike Toole
OSD/SDIO/T/DE
The Pentagon
Washington, DC 20301-7100

LTC Lanny Larson
OSD/SDIO/T/SK
The Pentagon
Washington, DC 20301-7100

Maj. Dan Allred
DNA/RAEV
6801 Telegraph Road
Alexandria, VA 22310

US Army Strategic Defense Command
Attn: CSSD-H-DN, Dan Whitener
P.O. Box 1500
Huntsville, AL 35807-3801

US Army Strategic Defense Command
Attn: CSSD-H-LK, Dr. Larry Atha
P.O. Box 1500
Huntsville, AL 35807-3801

US Army Strategic Defense Command
Attn: CSSD-H-Y, Bill Watt
P.O. Box 1500
Huntsville, AL 35807-3801

Nelson J. Wilson
SLCET-MW
USA LABCOM
Fort Monmouth, NJ 07703-5302

Dr. Richard R. Weiss
Astronautics Laboratory/CC
Edwards AFB, CA 93523

Don Hesketh
Astronautics Laboratory/LSN
Edwards AFB, CA 93523

Dr. Earl Good
Geophysics Laboratory - Code OP
Hanscom AFB
Bedford, MA 01731

Rita Sagalyn
Geophysics Laboratory - Code PH
Hanscom AFB
Bedford, MA 01731

David Cooke
AFGL/PHK
Hanscom AFB
Bedford, MA 01731

Dr. Charles Terrell
WL/AWY
Kirtland AFB, NM 87117

Capt Carol Moreland
Bldg 106
RADC/OCSE
Griffis AFB, NY 13441-5700

L.D. Massie
WRDC/POOC
Wright-Patterson AFB, OH 45433

Dr. Vickie Cox
AFATL/SAI
Eglin AFB, FL 32542

Dr. P.J. Palmadesso
Code 4700.3
Naval Research Laboratory
Washington, Dc 20375-5000

JHU Applied Physics Laboratory
Dr. Ching Meng (47-116)
Johns Hopkins Road
Laurel, MD 20707

Dr. Marsha Torr
MS ES51
Marshall Space Flight Center
Huntsville, AL 35812

Dr. Francis J. Brock
7 Tom Jones Court
Hampton, VA 23666

Dr. Carolyn K. Purvis
NASA Lewis Research Center
MS 302-1
21000 Brookpark Road
Cleveland, OH 44135

Dr. Larry Diehl
NASA Lewis Research Center
MS 500-200
21000 Brookpark Road
Cleveland, OH 44135

R.J. Sovie
NASA Lewis Research Center
MS 301-5
21000 Brookpark Road
Cleveland, OH 44135

John Smith
NASA Lewis Research Center
MS 301-5
21000 Brookpark Road
Cleveland, OH 44135

Dennis Connolly
NASA Lewis Research Center
MS 54-1
21000 Brookpark Road
Cleveland, OH 44135

Ira Myers
NASA Lewis Research Center
MS 301-3
21000 Brookpark Road
Cleveland, OH 44135

Robert Bercaw
NASA Lewis Research Center
MS 301-2
21000 Brookpark Road
Cleveland, OH 44135

Dr. Lubert Leger
MS ES-5
NASA Johnson Space Center
Houston, TX 77058

Dr. Gerry Murphy
Jet Propulsion Laboratory
4800 Oak Grove Drive
Pasadena, CA 91109

Dean Rovang
Sandia National Laboratories
P.O. Box 5800, MS 6511
Albuquerque, NM 87185

Dr. Don Reid
Mail Stop H804
Los Alamos National Laboratory
Los Alamos, NM 87545

Dr. Robert Hardekopf
Mail Stop H804
Los Alamos National Laboratory
Los Alamos, NM 87545

Dr. George Auchampaugh
ESS8, Mail Stop D438
Los Alamos National Laboratory
Los Alamos, NM 87545

Dr. Ron Smith
Mail Stop E561
Los Alamos National Laboratory
Los Alamos, NM 87545

Mike Thout
Mail Stop H820
Los Alamos National Laboratory
Los Alamos, NM 87545

Dr. Dave Bond
AEDC/DOFS
Arnold AFB, TN 37389

Dr. Michael Rigdon
IDA
1801 N. Beauregard Street
Alexandria, VA 22311

Dr. George Widhopf
MS M4-965
The Aerospace Corporation
2350 East El Segundo Blvd
El Segundo, CA 90245-4691

Dr. Ron Cohen
MS M5-754
The Aerospace Corporation
2350 East El Segundo Blvd
El Segundo, CA 90245-4691

Dr. Graham Arnold
MS M2-271
The Aerospace Corporation
2350 East El Segundo Blvd.
El Segundo, CA 90245-4691

Dr. Rohn Herm
MS M2-251
The Aerospace Corporation
2350 East El Segundo Blvd
El Segundo, CA 90245-4691

Dr. Stanley Shumilla
Mitre Corp, MS F301
Burlington Road
Bedford, MA 01730-0208

Dr. Joseph Barfield
P.O. Dwr 28510
Southwest Research Institute
San Antonio, TX 78284

Physical Sciences, Inc
Attn: Dr. Herb Cohen
Research Park, P.O. Box 3100
Andover, MA 01810

JAYCOR
Attn: Hank Klein
11011 Torreyana Road
P.O. Box 85154
San Diego, CA 92138

Ray Ratanen
Science & Engineering Assoc.
6535 S. Dayton Street
Englewood, CO 80111

McDonnell Douglas Space Systems Co.
Attn: Tim Shumate, MS 11/2
5301 Bolsa Avenue
Huntington Beach, CA 92647

Dr. Adam T. Drobot
SAIC, MS 2-3-1
1710 Goodrich Drive
McLean, VA 22102

Ron Hoffman
SAIC, Suite 2190
1875 Century Park East
Los Angeles, CA 90067

Dr. Wen Chiu
Bldg 21, MS 20Y05
General Electric Astro-Space
P.O. Box 8555
Philadelphia, PA 19101

Martin Marietta Astronautics
Attn: Mike Dougherty
MS DC4731
P.O. Box 179
Denver, CO 80201

Martin Marietta Astronautics
Attn: James R. Hoagland, MS 0301
P.O. Box 179
Denver, CO 80201

Dr. Robert J. Kraus
W.J. Schafer Assoc., Inc
1901 N. Ft. Meyer Drive
Suite 800
Arlington, VA 22209

Dr. David C. Straw
W.J. Schafer Assoc., Inc.
2000 Randolph Road, S.E.
Suite 205
Albuquerque, NM 87106

Dr. Keith Shillito
W.J. Schafer Assoc., Inc
2000 Liberty Plaza
Rome, NY 13440

Dr. Bruce Miller
Titan/Spectrum
2017 Yale Blvd, SE
Albuquerque, NM 87106

Dr. Ira Katz
S-CUBED
P.O. Box 1620
LaJolla, CA 92038-1620

Robert L. Hammel
TRW Space & Technology Group
One Space Park, MS R4/2190
Redondo Beach, CA 90278

Lockheed Missile & Space Co., Inc
Attn: Eric Laursen, 057-50B/529
1111 Lockheed Way
Sunnyvale, CA 94089

Boeing Aerospace Company
Attn: Dr. Paul Von Bech, MS 1E-09
P.O. Box 3999
Seattle, WA 98124-2499

Boeing Aerospace Company
Attn: John Adansky, MS 1E86
P.O. Box 3999
Seattle, WA 98124

Dr. David H. Berwald
Grumman Space Systems
Bethpage, NY 11714-3588

Dr. Edward J. Britt
Space Power Inc.
621 River Oaks Parkway
San Jose, CA 95134

Gerald A. Ouellette
G.A. Ouellette, Consulting
22 Warburton Way
Northhampton, MA 01060

Dr. Bill Nunnally
Power Conditioning Laboratory
University of Texas
Box 9016
Arlington, TX 76019

Dr. Erich Kunhardt
Ionized Gas Laboratory
PINY, Route 110
Farmingdale, NY 11735

Dr. Lynn Hatfield
Department of Physics
Texas Tech University
Lubbock, TX 79409

Dr. Will Kurth
Dept. of Physics & Astronomy
University of Iowa
Iowa City, IA 52242

R.C. Olsen
Physics Dept., MC 61-OS
Naval Post Graduate School
Monterrey, CA 93943

Dr. John Raitt
Center for Atmospheric & Space
Sciences
Utah State University
Logan, UT 84322-4405

Dr. Dennis Papadopoulis
Dept of Physics & Astronomy
University of Maryland
College Park, MD 20742

Dr. Douglas Torr
Research Institute, Rm C10
University of Alabama, Hunstville
Huntsville, AL 35899

Dr. Lloyd Gordon
Space Power Institute
231 Leach Center
Auburn University, AL 36849

Dr. M. Frank Rose
Director, Space Power Institute
231 Leach Center
Auburn University, AL 36849

CODE 1220

1 COPY

Do NOT make labels for these two-below:
Records---(1 copy)
Code 2628 (22 cys)

Director of Research
U.S. Naval Academy
Annapolis, MD 21402
(2 copies)

Naval Research Laboratory
Washinton, DC 20375-5000
Code 1220